Atmospheric methane and carbon dioxide from SCIAMACHY satellite data: initial comparison with chemistry and transport models

M. Buchwitz, R. de Beek, J. P. Burrows, H. Bovensmann, T. Warneke, J. Notholt, J. F. Meirink, A. P. H. Goede, P. Bergamaschi, S. Körner, et al.

Atmos. Chem. Phys. Discuss., 4, 7217–7279, 2004
www.atmos-chem-phys.org/acpd/4/7217/
SRef-ID: 1680-7375/acpd/2004-4-7217

Atmospheric Chemistry and Physics Discussions

Atmospheric methane and carbon dioxide from SCIAMACHY satellite data: initial comparison with chemistry and transport models

M. Buchwitz[1], R. de Beek[1], J. P. Burrows[1], H. Bovensmann[1], T. Warneke[1], J. Notholt[1], J. F. Meirink[2], A. P. H. Goede[2], P. Bergamaschi[3], S. Körner[4], M. Heimann[4], J.-F. Muller[5], and A. Schulz[6]

[1]Institute of Environmental Physics (IUP), University of Bremen FB1, Bremen, Germany
[2]Royal Netherlands Meteorological Institute (KNMI), Utrecht, The Netherlands
[3]Institute for Environment and Sustainability, Joint Research Centre (EC-JRC-IES), Ispra, Italy
[4]Max Planck Institute for Biogeochemistry (MPI-BGC), Jena, Germany
[5]Belgian Institute for Space Aeronomy (BIRA-IASB), Brussels, Belgium
[6]Alfred Wegener Institute (AWI), Potsdam, Germany

Received: 5 July 2004 – Accepted: 1 September 2004 – Published: 5 November 2004

Correspondence to: M. Buchwitz (Michael.Buchwitz@iup.physik.uni-bremen.de)

Abstract

The remote sensing of the atmospheric greenhouse gases methane (CH_4) and carbon dioxide (CO_2) in the troposphere from instrumentation aboard satellites is a new area of research. In this manuscript, results obtained from observations of the upwelling radiation in the near-infrared by SCIAMACHY (Scanning Imaging Absorption spectroMeter for Atmospheric CHartographY), which flies on board ENVISAT, are presented. Vertical columns of CH_4, CO_2 and oxygen (O_2) have been retrieved and the (air or) O_2-normalized CH_4 and CO_2 column amounts, the dry air column averaged mixing ratios XCH_4 and XCO_2 derived. In this manuscript the first results, obtained by using the version 0.4 of the Weighting Function Modified (WFM) DOAS retrieval algorithm applied to SCIAMACHY data, are described and compared with global models. This is an important step in assessing the quality and information content of the data products derived from SCIAMACHY observations. This study investigates the behaviour of CO_2 and CH_4 in the period from January to October 2003. The SCIAMACHY greenhouse gas column amounts and their mixing ratios for cloud free scenes over land are shown to be in reasonable agreement with models. Over the ocean, as a result of the lower surface spectral reflectance and resultant low signal to noise with the exception of sun glint conditions, the accuracy of the individual data products is poorer. The measured methane column amounts agree with the model columns within a few percent. The inter-hemispheric difference of the methane mixing ratios, determined from single day cloud free measurements over land, is in the range 30–110 ppbv and in reasonable agreement with the corresponding model data (48–71 ppbv). For the set of individual measurements the standard deviations of the difference with respect to the models are in the range ~100–200 ppbv (5–10%) and ±14.4 ppmv (3.9%) for XCH_4 and XCO_2, respectively. The XCO_2 model field in January shows low CO_2 concentrations over a spatially extended CO_2 sink region located in southern tropical/sub-tropical Africa. The SCIAMACHY data products also show low CO_2 mixing ratios over this area. The measured depth of the "CO_2 hole" in the region covering Zambia and the Congo basin

ACPD

4, 7217–7279, 2004

is, however, significantly larger (~20 ppmv) than in the model (~5 ppmv). The model indicates that the sink region becomes a source region about six months later and exhibits higher mixing ratios. The SCIAMACHY and the model data show a similar time dependence of the column mixing ratios over the period from January to October 2003. The amplitude of the difference between the maximum and the minimum for the SCIAMACHY data is, however, about a factor of four larger than that of the model. These results indicate that for the first time a regional CO_2 surface source/sink region has been detected by measurements from space.

1. Introduction

A prerequisite for reliable predictions of future atmospheric greenhouse gas amounts is an adequate understanding of the temporal and spatial behaviour of the surface sources and sinks and their response to climate change. Our understanding of the spatial distribution and temporal evolution of atmospheric methane and carbon dioxide is limited by our current knowledge of their sources and sinks: their variability being a significant source of uncertainty (see, e.g. Houweling et al., 1999; Gurney et al., 2002, and references given therein). Our knowledge about the spatial and temporal pattern of sources and sinks of CH_4 and CO_2 stems in large part from the inverse modelling of the in-situ measurements of a highly accurate but rather sparse network of surface stations (e.g. NOAA/CMDL). The results, obtained at scales of continents and oceanic basins, yield annual source/sink strengths with significant uncertainty (on the order of 100% for many regions)(Houweling et al., 1999; Gurney et al., 2002).

Retrievals of the amounts and distributions from spaced based remote sensing instrumentation have the potential to overcome the limitations of the surface network. This, however, requires high accuracy and precision. Rayner and O'Brian (2001) conclude that for CO_2 a precision of 2.5 ppmv (~0.7%) for monthly averaged column data at $8 \times 10^{\circ}$ spatial resolution is needed for a performance comparable to the current network of ground stations. Similar conclusions have been drawn by other studies, e.g.

ACPD
4, 7217–7279, 2004

Houweling et al. (2003), where measurements by the SCIAMACHY instrument are taken into account in estimating regional CO_2 source/sink uncertainty reductions. For methane such detailed studies are currently not available but similar requirements are to be expected.

Measuring CH_4 and CO_2 from space is a new research area and only a few relevant studies exist. Chedin et al. (2003) reported recently on their retrieval of mid-tropospheric CO_2 concentrations in the tropical region (20° N–20° S) derived from TOVS/NOAA-10 observations.

The first global maps of CH_4 columns have been retrieved from IMG/ADEOS thermal infrared (TIR) nadir spectra (Kobayashi et al., 1999a,b; Clerbaux et al., 2003). The results show qualitatively the expected variability, for example the North-South hemispheric gradient but also have some limitations, related to the retrieval algorithm (Clerbaux et al., 2003). The CH_4 and CO_2 amounts retrieved from TIR nadir observations have their maximum sensitivity in the middle troposphere and are relatively insensitive to the lower troposphere, due to the lack of thermal contrast. However many of the sources and sinks of CH_4 and CO_2 are located in the boundary layer, thus the modulation of the mxing ratios of these gases resulting from regional sources and sinks is most significant in the boundary layer. The SCIAMACHY near-infrared (NIR) nadir measurements are highly sensitive to concentration changes at all altitude levels, including the boundary layer. As absorption is measured, the measurements are sensitive to the column in a given altitude range rather than the mixing ratio. This is also true for the near-infrared CH_4 measurements of the MOPITT instrument onboard EOS-Terra, which utilises gas correlation spectroscopy, but the CH_4 column data product of MOPITT has not yet been released (http://terra.nasa.gov/About/MOPITT/).

Vertical columns of atmospheric CH_4 and CO_2 are retrieved from nadir spectra of the up-welling radiance in the near-infrared spectral region, measured by the SCIAMACHY instrument. CH_4 and CO_2 have been retrieved respectively from the spectral regions 2265–2280 and 1558–1594 nm, which are relatively free from interfering absorbers. Simultaneously, oxygen (O_2) columns have been retrieved from the oxygen A band

ACPD
4, 7217–7279, 2004

(around 760 nm). This enables the dry air column averaged mixing ratios, denoted as XCH_4 and XCO_2, to be determined: XCH_4:=CH_4-column/O_2-column×0.2095, where 0.2095 is the O_2 mixing ratio of dry air (XCO_2 is defined analogously).

A subset of the SCIAMACHY data products discussed in this paper has been compared with Fourier Transform Spectroscopy (FTS) solar occultation measurements obtained during a cruise of the German research vessel Polarstern from Cape Town to Bremerhaven in January/February 2003 (Warneke et al., submitted, 2004[1]) (the ship track is shown in Figs. 22 and 25). In that study agreement within ∼5% has been found for measurements over land (Africa). For the SCIAMACHY measurements over the Atlantic Ocean (closer to the ship track) larger deviations (scatter) are found. This is expected because of the low surface spectral reflectance of the ocean and the resultant low signal-to-noise ratio for the spectra.

The CO_2 and CH_4 data products have been compared with global models of atmospheric transport and chemistry. This is an important step in assessing the quality of the data products: validation by comparison with independent measurements being limited by the number of ground stations.

The WFM-DOAS v0.4 methane and carbon dioxide columns and models, discussed in this manuscript, are planned in the longer term to be used to infer information about the surface sources and sinks of the greenhouse gases CH_4 and CO_2 (e.g. within the European Commission 5th framework research project EVERGREEN, see http://www.knmi.nl/evergreen) by means of inverse modelling. Because the surface sources and sinks only result in a weak modulation of the background columns, this application requires high accuray and precision (see discussion given above).

[1]Warneke, T., de Beek, R., Buchwitz, M., Notholt, J., Schulz, A., Velazco, V., and Schrems, O.: Shipborne solar absorption measurements of CO_2, CH_4, N_2O and CO and comparison with SCIAMACHY WFM-DOAS retrievals, Atmos. Chem. Phys. Discuss., submitted, 2004.

ACPD
4, 7217–7279, 2004

2. The SCIAMACHY instrument

The SCanning Imaging Absorption spectroMeter for Atmospheric CHartographY (SCIAMACHY) instrument (Burrows et al., 1995; Bovensmann et al., 1999, 2004) is part of the atmospheric chemistry payload of the European Space Agencies (ESA) environmental satellite ENVISAT, launched in March 2002. The SCIAMACHY objectives and instrument concept were developed between 1984 and 1988 and proposed to ESA for flight on the ESA polar platform in July 1988, subsequently renamed ENVISAT. This proposal was supported by the German space agency (DLR). In February 1989, SCIAMACHY was selected as a national contribution after peer review for its Phase A study. Subsequently the relevant Dutch and Belgian space agencies, joined the consortium developing and providing SCIAMACHY to ESA for ENVISAT.

ENVISAT flies in sun-synchronous polar low Earth orbit crossing the equator at 10:00 a.m. local time. SCIAMACHY is a grating spectrometer that measures spectra of scattered, reflected, and transmitted solar radiation in the spectral region 240-2400 nm in nadir, limb, and solar and lunar occultation viewing modes. The SCIAMACHY near-infrared (NIR) nadir spectra contain information about many important atmospheric trace gases such as CH_4, CO_2, CO, and N_2O.

For this study observations from channel 4 (for O_2), channel 6 (for CO_2) channel 8 (for CH_4), and Polarization Measurement Device (PMD) number 1 (~320–380 nm) have been used. Channels 4, 6 and 8 measure simultaneously the spectral regions 600–800 nm, 970–1772 nm and 2360–2385 nm at spectral resolutions of 0.4, 1.4 and 0.2 nm, respectively. For channel 8 data, the spatial resolution, i.e. the footprint size of a single nadir measurement, is $30\times120\,km^2$ corresponding to an integration time of 0.5 s, except at high solar zenith angles (e.g. polar regions in summer hemisphere), where the pixel size is twice as large ($30\times240\,km^2$). For channel 4 and 6 the integration time is smaller, i.e. 0.25 s, and corresponds to $30\times60\,km^2$. SCIAMACHY also performs direct (extraterrestrial) sun observations mainly to obtain the solar reference spectra needed for the retrieval. The in-flight optical performance of SCIAMACHY is overall as

ACPD
4, 7217–7279, 2004

expected from the on-ground calibration and characterization activities (Bovensmann et al., 2004). One exception is the time dependent optical throughput variation in the SCIAMACHY NIR channels 7 and 8 due to ice build-up. This effect is minimised by regular heating of the instrument (Bovensmann et al., 2004) and further discussed in Sect. 9.1.

3. Pre-processing of SCIAMACHY spectra

The SCIAMACHY spectra used for this study are the ENVISAT operational Level 1 data products. The calibration is currently not optimal (especially in the NIR). During the commissioning phase of ENVISAT in the first six months of the mission in space, the planned in-orbit dark signal measurement strategy was identified as being inadequate. As a result improved dark signal measurements began at the end of 2002. They are included in the Level 1 data products but are not used by the current version of the Level 0-1 processor. In this study, the binary Level 1 data files have been "patched", i.e. the standard dark signals have been replaced by the improved ones. This has resulted in significantly better WFM-DOAS fits, as expected. In order to further improve the calibration, non linearities in the analogue to digital converter (ADC) are taken into account (Kleipool, 2003).

Especially the channel 8 detector array is very inhomogeneous with respect to detector pixel properties, such as quantum efficiency and dark signal, which vary strongly from pixel to pixel. Thus bad and dead pixels are not included in data product retrieval. We have extended the "dead pixels mask" of the Level 1 data product to reject pixels, inducing strong spikes in the solar irradiance and/or nadir radiance spectra.

As the calibration of the solar reference spectra as contained in the Level 1 data products is also preliminary, a solar reference spectrum with an improved calibration has been used. This spectrum has been generated and made available by ESA (provided by J. Frerick, ESA/ESTEC).

ACPD
4, 7217–7279, 2004

4. The WFM-DOAS retrieval algorithm

The Weighting Function Modified Differential Optical Absorption Spectroscopy (WFM-DOAS) retrieval algorithm has been developed primarily for the retrieval of the total column amounts of CO, CH_4, CO_2, H_2O, and N_2O, from the SCIAMACHY NIR nadir spectra (Buchwitz et al., 2000a, 2004; Buchwitz and Burrows, 2004). WFM-DOAS, however, is not limited to this application and has also been successfully applied to ozone total column retrieval using GOME data (Coldewey-Egbers et al., 2004) and to water vapour retrieval using GOME and SCIAMACHY nadir spectra around 700 nm (Noël et al., 2004).

Any algorithm that aims at retrieving atmospheric information from global satellite data not only has to be accurate but also has to be sufficiently fast in order to be able to process huge amounts of data (SCIAMACHY spectra comprise about 8000 data points, which are recorded several times per second corresponding to a data rate of 400 kbit per second). Accuracy and speed are conflicting requirements and an appropriate compromise has to be found. The WFM-DOAS algorithm in its current implementation (look-up table approach) as described in this section is very fast. The processing of an entire orbit of pre-processed SCIAMACHY spectra (see Sect. 3) requires a couple of minutes per fitting window on a standard single processor PC, which is more than one order of magnitude faster than real time (one orbit lasts about 100 min).

WFM-DOAS is based on fitting the logarithm of a linearized radiative transfer model I^{mod} plus a low-order polynomial P to the logarithm of the ratio of a measured nadir radiance and solar irradiance spectrum, i.e. observed sun-normalized radiance I^{obs}. The linear least-squares WFM-DOAS equation can be written as follows (fit parameters are underlined):

$$\left\| \ln I_i^{obs} - \ln I_i^{mod}(\hat{\underline{\mathbf{V}}}) \right\|^2 \equiv \|RES_i\|^2 \rightarrow min. \quad (1)$$

where the linearized radiative transfer model is given by

$$\ln I_i^{mod}(\hat{\underline{\mathbf{V}}}) = \ln I_i^{mod}(\bar{\mathbf{V}}) \quad (2)$$

ACPD
4, 7217–7279, 2004

$$+ \quad \sum_{j=1}^{J} \frac{\partial \ln I_i^{mod}}{\partial V_j}\bigg|_{\bar{V}_j} \times (\hat{V}_j - \bar{V}_j) + P_i(a_m).$$

Index i refers to the center wavelength λ_i of detector pixel number i. The components of vectors $\boldsymbol{V}$, denoted V_j, are the vertical columns of all trace gases which have absorption lines in the selected spectral fitting window. The fit parameters are the desired trace gas vertical columns $\hat{V}_j$ and the polynomial coefficients a_m. An additional fit parameters also used (but omitted in Eqs. 1 and 2) is the shift (in Kelvin) of a pre-selected temperature profile. This fit parameter has been added in order to take the temperature dependence of the trace gas absorption cross-sections into account. The fit parameter values are determined by minimizing (in a linear least-squares sense) the difference between observation ($\ln I_i^{obs}$) and WFM-DOAS model ($\ln I_i^{mod}$), i.e. fit residuum RES_i, for all spectral points λ_i simultaneously. A derivative, or weighting function, with respect to a vertical column refers to the change of the top-of-atmosphere radiance caused by a change (here: scaling) of a pre-selected trace gas vertical profile. The WFM-DOAS reference spectra are the logarithm of the sun-normalized radiance and its derivatives. They are computed with a radiative transfer model (Buchwitz et al., 2000b) for assumed (e.g. climatological) "mean" columns $\bar{\mathbf{V}}$. Multiple scattering is fully taken into account. The least-squares problem (Eqs. 1 and 2) can also be expressed in the following vector/matrix notation: Minimize $\|\mathbf{y}-\mathbf{A}\,\mathbf{x}\|^2$ with respect to $\mathbf{x}$. The solution is $\hat{\mathbf{x}}=\mathbf{C_x}\mathbf{A}^T\mathbf{y}$ where $\mathbf{C_x}\equiv(\mathbf{A}^T\mathbf{A})^{-1}$ is the covariance matrix of solution $\hat{\mathbf{x}}$. The errors of the retrieved columns are estimated as follows (Press et al., 1992): $\sigma_{\hat{V}_j}=\sqrt{(\mathbf{C_x})_{jj}\times\sum_i RES_i^2/(m-n)}$, where $(\mathbf{C_x})_{jj}$ is the j-th diagonal element of the covariance matrix, m is the number of spectral points in the fitting window and n is the number of linear fit parameters (RES_i is the spectral fit residuum, see Eq. 1).

In order to avoid time consuming on-line radiative transfer simulations, a look-up table approach has been implemented (see Buchwitz and Burrows, 2004, for details). The WFM-DOAS reference spectra (radiance and derivatives) have been computed for

ACPD
4, 7217–7279, 2004

cloud free conditions assuming a US Standard Atmosphere, a tropospheric maritime and stratospheric background aerosol scenario and a surface albedo of 0.1. They depend on solar zenith angle, surface elevation (0–3 km in steps of 1 km), and water vapor column. An error analysis has been performed by applying WFM-DOAS to simulated nadir spectra (Buchwitz and Burrows, 2004; Buchwitz et al., 2000a). The CH_4 and CO_2 column retrieval random errors (precision) due to instrument noise are ∼1% (1-sigma) for the spectral fitting window used for this study (solar zenith angle 50°, albedo 0.1). The more systematic errors introduced by, e.g. the currently implemented look-up table scheme, are typically less than a few percent for all cases investigated, covering error sources such as the variability of temperature and water vapour profiles, aerosols, sub-visual cirrus clouds, and albedo effects.

An error source not discussed in detail in Buchwitz and Burrows (2004) is the influence of the pressure profile on the retrieved columns. If an incorrect pressure profile is used for the retrieval an error is introduced because the absorption cross sections (line shapes) of the trace gases depend on pressure. This influences the retrieval although the spectral resolution of SCIAMACHY is typically not high enough to resolve individual lines. Figure 1 shows CO_2, CH_4, and O_2 columns as retrieved from SCIAMACHY for a cloud free scene near Senegal, Africa, on January 23, 2003. The columns are plotted as a function of the ground height of the corresponding nadir ground pixels (height above sea level obtained from a surface topography database). For a standard pressure profile the pressure drops by about 1.2% per 100 m altitude increase. This corresponds to an air column decrease of 1.2% per 100 m ground pixel height increase. For the relatively long-lived and therefore well-mixed gases CH_4 and CO_2 this also corresponds to a column decrease of ∼1.2% per 100 m altitude increase. Figure 1 shows that this can in fact be observed with SCIAMACHY to a high degree of accuracy. This demonstrates the theoretically predicted sensitivity of SCIAMACHY to small (partial column) changes in the lower troposphere.

Figure 1, however, also shows that the slope of the retrieved columns as a function of surface elevation is somewhat steeper than expected (green line). This can be

ACPD
4, 7217–7279, 2004

explained by the fact that a constant (US Standard Atmosphere) pressure profile is currently used in WFM-DOAS in combination with a look-up table that includes different surface elevations but only on a coarse grid (0, 1, 2, and 3 km). A simple next neighbour approach is currently used to select the (radiance and derivatives) reference spectra for a given ground pixel. Therefore, for ground pixels with an average surface elevation of less than 500 m (as shown in Fig. 1) identical WFM-DOAS reference spectra are currently used (except for solar zenith angle interpolation). They have all been computed assuming a standard pressure profile with 1013 hPa at the lowest level. The advantage of this approach (apart from the fact that the look-up table is relatively small) is that the variability of the retrieved columns, e.g. the variability shown in Fig. 1, is entirely due to the spectral measurements of SCIAMACHY. Because all the reference spectra are identical it is thereby ensured that no artificial variability is mixed into the measured (!) columns by using a priori information in the retrieval process. The red lines shown in Fig. 1 have been determined by applying WFM-DOAS to simulated measurements computed with the same profiles (including the pressure profile) as used for the generation of the look-up table but with a lower boundary equal to the surface elevation of the corresponding ground pixels. As can be seen, the nearly linear dependence of the retrieved columns and mixing ratios on the surface elevation is better represented by the slopes of the corresponding red lines than by the slopes of the green lines. This shows that the "slope error" seen in Fig. 1 can in fact be explained by the use of a constant pressure profile. This error source needs to be minimized in future versions of WFM-DOAS. This, however, is not trivial if one wants to avoid the use of highly correlated a priori information (meteorological analysis, surface topography) with errors on the order of (or even significantly larger than the weak) the signal to be detected.

It is also important to point out that no a priori information is used to constrain the retrieved columns. As explained, a priori information on the atmosphere is only used to get a reasonable linearization point for the unconstrained linear least-squares WFM-DOAS fit.

ACPD
4, 7217–7279, 2004

5. Sensitivity to boundary layer CH_4 and CO_2

One significant advantage of the near-IR spectral region, in contrast to, e.g. the thermal IR region, for the detection of greenhouse gas columns is that the radiation detected by a nadir viewing satellite instrument is highly sensitive to trace gas concentration changes in the boundary layer. This is important as the concentration variation due to sources and sinks is largest in the lower troposphere and, therefore, this region must be probed in order to get accurate information on surface sources and sinks.

This sensitivity is theoretically demonstrated for SCIAMACHY CH_4 and CO_2 observations, by computing the CH_4 and CO_2 vertical column averaging kernels, which are shown in Figs. 2 and 3. For this purpose WFM-DOAS has been applied to simulated nadir spectra generated for an unperturbed as well as for perturbed greenhouse gas profiles. A perturbed CH_4 or CO_2 profile has been generated from the unperturbed profiles by adding a certain (constant) number of CH_4 or CO_2 molecules at a given altitude level. The averaging kernels (AK) are defined as follows: $AK(z) \equiv (V^{rp} - V^{tu})/(V^{tp} - V^{tu})$, where V^{tu} is the true greenhouse column for the unperturbed greenhouse profile, and V^{tp} and V^{rp} are the true and retrieved columns of the perturbed profiles (having an enhanced greenhouse gas concentration at altitude z), respectively. The true column V^{tu} is the column of the standard model atmosphere. To illustrate this: A value of the column averaging kernel of 1.2 at 5 km means that if, for example, 100 molecules (per volume element) are added at 5 km (to the standard profile), 120 additional molecules are retrieved, which is an overestimation of 20% (not of the total column but) of the difference between the true profile and the standard (or a priori) profile. If the true profile has lower values than the standard profile the retrieved column will be underestimated accordingly.

In order not to introduce any errors when calculating the averaging kernels WFM-DOAS has also been applied to spectra computed for the standard model atmosphere and it has been verified that the retrieved column agrees (within better than 0.05%) with the true column of the unperturbed model atmosphere, i.e. V^{tu}.

ACPD
4, 7217–7279, 2004

Due to the fact that the SCIAMACHY averaging kernels are "imperfect" in the sense that they deviate from unity, a so-called smoothing error will result for the retrieved columns. This smoothing error has been estimated by Connor et al. (2003) for the CO_2 measurements of SCIAMACHY and other instruments using an optimal estimation retrieval algorithm. For SCIAMACHY the estimated CO_2 column smoothing error is 0.5 ppmv (the results for the other instruments are: AIRS on Aura: 1.5 ppmv, planned OCO instrument: 0.3 ppmv, ground based FTS: 0.01 ppmv).

For altitudes where the averaging kernels are significantly larger than zero (where they are on the order of 1.0) the measurement system, here SCIAMACHY, is sensitive to concentration changes. In this context it has to be noted that the exact value of the averaging kernel not only depends on the instrument but also on the retrieval algorithm. The averaging kernels shown here are valid for the WFM-DOAS algorithm as used for this study. They will be different for different algorithms (i.e. WFM-DOAS, which is based on scaling entire profiles, has other averaging kernels than, for example, an optimal estimation profile retrieval algorithm, which has more degrees of freedom). These remarks refer to the details of the averaging kernels, not however to some general conclusions to be drawn here, e.g. about the sensitivity to the lower atmosphere. Those conclusions can be drawn more or less independent of what retrieval algorithm has been used. This is possible because the altitude sensitivity can (also) entirely be assessed without averaging kernels simply by calculating the derivative of the top of atmosphere radiance with respect to concentration changes at the altitudes of interest. This has been done for this study and the results (not shown here) are consistent with the averaging kernels shown in Figs. 2 and 3. These derivatives also show, for example, the typical decrease of the sensitivity with altitude (the altitude where the molecules have been added) as shown in Figs. 2 and 3. This is typical for relatively strong absorption lines and is due to saturation of unresolved lines in the strong absorber limit (Goody and Yung, 1989) which gets more important the narrower (i.e. the less pressure broadened) the lines are.

The SCIAMACHY/WFM-DOAS averaging kernels for CH_4 and CO_2 shown in Figs. 2

ACPD
4, 7217–7279, 2004

and 3 indicate that the sensitivity of the SCIAMACHY nadir measurements for solar zenith angles less than ∼70° is high (larger than 0.5) at all altitudes below ∼100 hPa (∼16 km), including the boundary layer.

6. Cloud identification

The WFM-DOAS algorithm as described in Sect. 4 is strictly speaking only appropriate for cloud free scenes. As cloud contamination results in errors on the retrieved total columns it is important to at least identify the cloud free pixels. For this purpose a cloud mask is generated (0: pixel probably cloud free, 1: pixel probably cloud contaminated).

Currently, this cloud mask is generated using the sub-pixel information provided by SCIAMACHY's Polarisation Measurement Device (PMD) number 1 covering approximately the spectral region 320–380 nm (Bovensmann et al., 1999). A simple single threshold algorithm is used. This algorithm does not specifically detect clouds but enhanced UV backscatter which results from clouds but also from enhanced aersols and higher than average surface reflectivity (e.g. due to ice and snow). The algorithm works as follows: First, each interpolated PMD 1 readout as contained in the Level 1 file (32 values per one second integration time) that corresponds to a given (main channel) ground pixel is divided by the cosine of the solar zenith angle to obtain a quantity approximately proportional to top-of-atmosphere reflectivity. If this "PMD 1 reflectivity" is higher than a pre-defined threshold the corresponding sub-pixel is assumed to be cloud contaminated. A (main channel) ground pixel is flagged cloud contaminated if one or more of its PMD sub-pixels is cloud contaminated.

PMD 1 has been selected for the cloud mask generation because the scattered and reflected solar UV radiation detected by SCIAMACHY's nadir mode penetrates deep into the atmosphere (that is, the average scattering height is located close to the Earth surface) but the sensitivity to the Earth surface is significantly lower than for the other PMD channels covering parts of the visible and NIR spectral regions because scattering in the atmosphere decreases with increasing wavelength. This effect can

ACPD
4, 7217–7279, 2004

be seen when comparing global maps showing the signal of the various PMDs. For example, a land to sea contrast is (nearly) not visible for PMD 1 but clearly visible for the other PMDs (not shown here). The optimum threshold has been determined empirically by visual inspection of global maps of PMD 1 reflectivities overlayed with cloud masks generated for various thresholds. As an example, Fig. 4 shows a PMD 1 map for 24 January 2003.

7. Methane and carbon dioxide WFM-DOAS fits

Figures 5 and 6 show typical CH_4 and CO_2 WFM-DOAS fits. For CH_4 a small spectral fitting window in SCIAMACHY channel 8 is used and for CO_2 a small fitting window in channel 6. As can be seen, the spectral absorption structures of both gases are clearly visible in the SCIAMACHY data and good fits to the methane and carbon dioxide absorption bands have been obtained. The root-mean-square (RMS) difference between the WFM-DOAS model and the SCIAMACHY measurement is 1.7% for the example shown in Fig. 5 and 0.7% for the CO_2 fit shown in Fig. 6.

The fit residuals, i.e. the difference spectra between measurement and model (as shown in the bottom panel of Fig. 6) are not yet signal-to-noise limited but are dominated by rather stable spectral artifacts. This needs further investigation, e.g. by analysing time series, but is most probably due to a combination of various errors such as errors in the spectroscopic data (Rothman et al., 2003), errors due to the still preliminary calibration of the SCIAMACHY nadir and solar spectra, and spectrometer slit function uncertainties. Probably as a result of this the CO_2 and O_2 columns initially retrieved showed a significant bias, namely a systematic underestimation of the CO_2 columns and an overestimation of the O_2 columns (the mixing ratios of these gases are quite well known and do not vary very much; therefore a good estimate of their columns for a given location can be made even without any SCIAMACHY measurement). In order to roughly compensate for this, constant (i.e. space and time independent) scaling factors have been applied to all WFM-DOAS version 0.4 CO_2 and O_2 columns shown

ACPD
4, 7217–7279, 2004

in this study. These scaling factors are 1.27 for the CO_2 columns and 0.85 for the O_2 columns. All columns have simply been multiplied with these factor (and this transformation can simply be reversed, if considered necessary, by dividing all WFM-DOAS version 0.4 columns by these numbers). Scaling factors of that order have also been used in other studies. For example, Yang et al. (2002) applied a scaling factor of 1.058 to their XCO_2 measurements. The WFM-DOAS version 0.4 CH_4 columns have not been scaled. This scaling factor issue needs further study and we hope that in the future we do not need the scaling factors any more. At this point, however, it is important to point out that the focus of this study is to investigate to what extent atmospheric variability can be detected with SCIAMACHY (because this is where the information on sources and sinks will come from). The absolute level of the columns is only of minor importance for most of the scientific applications.

8. Global models of chemistry and transport

In this section a short description the global models of chemistry and transport used in the study is given. Four different models have been used, three for the methane comparison (TM3 model of KNMI, TM5 model of JRC, and the IMAGES model of IASB) and one for the comparison of carbon dioxide (TM3 model of MPI-BGC).

8.1. TM3 model of KNMI

TM3 is a global offline chemistry-transport model driven by meteorological fields from the ECMWF weather forecast model. The model is run on a resolution of 3×2° and 31 vertical layers. The version applied here is basically the same as described in Lelieveld and Dentener (2000), except that CH_4 emissions are included following Houweling et al. (1999) and scaled to a yearly global total of 590 Tg. CH_4 at the top of the model domain (10 hPa) is nudged to HALOE/CLAES satellite data.

8.2. TM5 model of JRC

The TM5 model is a two-way nested atmospheric zoom model (Krol et al., 2004). It allows to define zoom regions (e.g. over Europe) which are run at higher spatial resolution (1×1°), embedded into the global domain, run at a resolution of 6×4°. We employ the tropospheric standard version of TM5 with 25 vertical layers. TM5 is an offline model and uses analysed meteorological fields from the ECMWF weather forecast model to describe advection and vertical mixing by cumulus convection and turbulent diffusion. CH_4 emissions are as described by Bergamaschi et al. (2004) (a priori emissions). Chemical destruction of CH_4 by OH radicals is simulated using pre-calculated OH fields based on CBM-4 chemistry and optimized with methyl chloroform, for the stratosphere also the reaction of CH_4 with Cl and $O(^1D)$ radicals are considered.

8.3. IMAGES model of IASB

IMAGES is a global chemistry-transport model describing the evolution of 60 chemical compounds at a resolution of 5×5° with 25 levels between the surface and a pressure of 50 hPa. It uses monthly averaged meteorological fields obtained from a 5-year ECMWF climatology. Advection is solved using the semi-Lagrangian approach, whereas deep convection and planetary boundary layer (PBL) mixing are parameterized. The effect of wind variability at short time scales is accounted using horizontal diffusion coefficient estimated from the ECMWF wind variances. Emission fields are adapted from Muller and Brasseur (1995). Global annual emissions of CH_4 amount to 514 Tg/year.

8.4. TM3 model of MPI-BGC

TM3 3.8 (Heimann and Körner, 2003) is a three-dimensional global atmospheric transport model for an arbitrary number of active or passive tracers. It uses re-analyzed meteorological fields from the National Center for Environmental Prediction (NCEP) or from the ECMWF re-analysis. The modelled processes comprise tracer advection,

vertical transport due to convective clouds and turbulent vertical transport by diffusion. Available horizontal resolutions range from 8×10° to 1.1×1.1°. In this case, TM3 was run with a resolution of 1.8×1.8° and 28 layers, and the meteorology fields were derived from the NCEP/DOE AMIP-II reanalysis. CO_2 source/sink fields originate from Takahashi et al. (2002), the EDGAR 3.2 database and from biosphere fluxes obtained by the model BIOME-BGC.

9. Comparison of SCIAMACHY data with models

In order to facilitate a quantitative comparison of the SCIAMACHY data with the model fields, all data have been gridded on a common 0.5×0.5° latitude/longitude grid. This corresponds to a grid box size of about 50×50 km^2 (except at high latitudes) which is on the order of the resolution of the SCIAMACHY ground pixels (CO_2: 30×60 km^2, CH_4: 30×120 km^2). The model grids are typically integer multiples of 0.5 degrees. This enables to map the model data onto the 0.5° grid without any interpolation. The only exception is the MPI-BGC/TM3 model. Here a bi-linear interpolation scheme has been used.

9.1. Methane columns and XCH_4

In this section SCIAMACHY data are compared with corresponding model data. Detailed results are presented for four days of the year 2003 (24 January, 28 March, 30 May, and 23 July). These days have been selected based on the several criteria with the main criterion being availability of all 14 daily ENVISAT orbits in consolidated Level 1b format (i.e. entire orbits including all the necessary auxillary data needed for calibration). Not all ENVISAT orbits have been processed and made available by ESA and only for a small number of days all 14 daily orbits were available for this study.

Figure 7 shows the methane vertical columns as retrieved from the SCIAMACHY measurements obtained on 24 January 2003. As described above, no cloud correction

is being performed by WFM-DOAS. The low columns (shown in blue) mainly correspond to cloud covered scenes. This was expected as typically only the column above a cloud is observed. This can be seen by comparing (the blue regions of) Fig. 7 with (the white regions of) Fig. 4. Only ground pixels with a methane column fit error of less than 10% are shown in Fig. 7, i.e. only pixels where a relatively good match of the WFM-DOAS model and the measurements has been achieved. Most of the rejected pixels (those having a fit error larger than 10%) are located over ocean. Except for sun-glint conditions the reflectivity of the ocean is low, especially at near-infrared wavelength. As a result, the signal detected by SCIAMACHY is low and, therefore, also the signal-to-noise ratio, resulting in spectral fits being significantly worse compared to fits over land.

Figure 8 shows the same columns as shown in Fig. 7 but restricted to cloud free pixels. These columns are compared with the corresponding KNMI/TM3 model columns shown in Fig. 9. As can be seen, the measured columns correspond quite well with the model columns. The lowest columns (blue) are located over the Himalaya region. This is primarily due to surface topography (the higher the average surface elevation of a ground pixels the lower the air mass above this pixel and the lower the column of a well-mixed gas). Over northern Africa the measured as well as the model columns are in the range 3.5–3.8×10^{19} molecules/cm^2. Over South America the columns are significantly lower (less than 3.4×10^{19} molecules/cm^2), especially over the Andes mountains. This is true for the measurements as well as for the model data. Over Australia the measured columns are around 3.7×10^{19} molecules/cm^2 which is a few percent higher than the model columns which are around 3.5×10^{19} molecules/cm^2.

Figure 10 shows the methane dry air column averaged mixing ratio XCH_4 as measured by SCIAMACHY for all ground pixels where the fit error is smaller than 10%. Figure 11 shows the same data but restricted to the cloud free pixels. Figure 12 shows the corresponding KNMI/TM3 model results. The color scale used for Fig. 12 is not exactly identical with the color scale used for Fig. 11 in order to better show the XCH_4 spatial pattern, which is somewhat "smoother" in the model compared to the mea-

ACPD
4, 7217–7279, 2004

surements. Figures 11 and 12 enable a comparison of the measured and modelled XCH_4. Overall, the pattern agree quite well. Both data sets show relatively high values in the northern hemisphere and relatively low values over South America. Over Australia the measured XCH_4 is about 1–2% higher (∼1.74 ppmv) compared to the model (∼1.70 ppmv). Differences on the order of 1–2% are also observed in other regions, e.g. over Mexico, where the measured XCH_4 is ∼1.72 ppmv and the model values are around ∼1.76 ppmv. The largest difference is observed over the Himalaya region, where the measured XCH_4 are about 10% higher than the model values.

Figures 13 and 14 show the corresponding JRC/TM5 and the IASB/IMAGES model XCH_4 fields. The color scale has been slightly adjusted to better see the spatial pattern. As can be seen, the XCH_4 pattern of the KNMI/TM3 and the JRC/TM5 models agree very well. Both models use the same meteorology (ECMWF), advection scheme and parameterisation of subgridscale vertical mixing. However, they are applied here in different resolutions (TM3: 3×2; TM5: 6×4, over Europe 1×1) and use different CH_4 emission inventories. A coupled European-global inversion based on the TM5 model has recently been performed by Bergamaschi et al. (2004), using high-precision ground-based in-situ measurements. The inversion, performed for year 2001, suggests e.g. higher emission from USA, Southern Africa, and India, and lower emission from Northern Africa, Russia and East Asia compared to the bottom-up inventory used in this study, with signicant influence on the simulated global CH4 distribution. For future comparisons of SCIAMACHY data we will use such optimized CH_4 simulations, representing a calibrated reference consistent with global in-situ observations. The XCH_4 field computed by the IASB/IMAGES model is simalar as those from the TM models, but significantly smoother because it uses monthly averaged meteorology. The somewhat lower mixing ratios calculated in the southern hemisphere reflect primarily a longer interhemispheric exchange time in this model compared to the TM models, as demonstrated by the steeper gradients around the ITCZ. In addition, the particularly low biomass burning emissions used in IMAGES (based on the emission ratios by Andreae and Merlet, 2001) might explain the absence of XCH_4 hot spots associated to

ACPD
4, 7217–7279, 2004

vegetation fires, e.g. over Australia and Northern Africa. It is planned to also use the IASB/IMAGES model for CH_4 inverse modelling but this requires monthly averages of the SCIAMACHY methane data not yet produced.

Figure 15 shows a comparison of the CH_4 columns as measured by SCIAMACHY (the same data are also shown in Fig. 8) with the corresponding columns of the KNMI/TM3 model. The comparison is restricted to cloud free measurements over land. As can be seen, both data sets correlate quite well. The linear correlation coefficient (Pearsons r) is 0.88.

Figure 16 shows the measured XCH_4 and the KNMI/TM3 model values as a function of latitude. As can be seen, the variability of the measured XCH_4 is significantly higher (~100 ppbv or 5%) than the model XCH_4 (~30 ppbv). The hemispheric averages of the SCIAMACHY data (red horizontal lines) agree quite well with the corresponding model values which have been computed using the same (latitude/longitude) grid boxes as used for SCIAMACHY. The difference between the hemispheric averages is the inter-hemispheric difference (IHD). The IHD as determined from the SCIAMACHY measurements on 24 January 2003, is 53 ppbv. The corresponding model value is 71 ppbv. Note that this model value has been determined taking into account the spatial sampling of SCIAMACHY and, therefore, is not identical with a model IHD computed from all model grid boxes. For this day a latitude of 10° south has been selected to "separate" the hemispheres. This latitude roughly corresponds to the (average) position of the intertropical convergence zone (ITCZ) in January as can be concluded from, e.g. Fig. 16, which shows a gap of SCIAMACHY measurements around −10° latitude due to large cloud cover (typical for the ITCZ) with higher than average methane mixing ratios north of this region and lower mixing ratios south of this latitude.

Figure 17 shows a similar plot as Fig. 16 but for the JRC/TM5 model. Here the agreement between the measured IHD (53 ppbv) and the corresponding model value (56 ppbv) is even better.

A similar analysis has also been performed for three others days of the year 2003. The results are summarized in Tables 1 and 2. These tables shows that the quantities

ACPD
4, 7217–7279, 2004

used to characterise the level of similarity between the measurement and the models (i.e. correlation coefficient, mean difference and standard deviation of the difference) are significantly different for the four days analysed. For example the correlation coefficient for the CH_4 columns is 0.88 on 24 January 2003, but as low as 0.55 on 30 March 2003. This can be explained, at least partially, by the fact that the correlation coefficient strongly depends on the range of columns observed which is primarily determined by the range of ground pixel surface pressures covered by cloud free pixels (on 24 January, for example, one orbit goes over the nearly cloud free Andes mountains, which is not the case for 30 March).

In this context it also has to be pointed out that the WFM-DOAS Version 0.4 retrieval scheme and related parameters (degree of the polynomial, slit function parameters, dead and bad detector pixel mask, solar reference spectrum, etc.) are identical for all days, i.e. the retrieval scheme is rather static. This might not be the optimum because certain time dependencies might need careful consideration, e.g. to take into account effects resulting from the time dependent ice-layer build up in SCIAMACHY's channel 8 (see Sect. 2) which has been used for CH_4 retrieval. The average channel 8 relative transmission is shown in the last column of Table 1. This transmission has been determined from ratios of solar (and internal calibration lamp) spectra as measured in-orbit by SCIAMACHY. The transmission values listed characterise the change of the transmission relative to the first in-orbit measurements. In order to bring this transmission back to its maximum value (of ∼1.0) SCIAMACHY (more precisely, its radiant cooler) is regularly heated ("decontamination") to get rid of the ice layer. After decontamination the transmission is close to 1.0 but decreases (roughly exponentially) with time. Table 1 shows that the transmission is highest (0.9) for 24 January 2003. For this day (a day shortly after a major decontamination phase) the comparison with the KNMI/TM3 model shows the best agreement (e.g. highest correlation coeffient, smallest standard deviation of the difference). For 28 March and 23 July the SCIAMACHY CH_4 columns are on average 10–15% lower than the model columns (whereas for the other days the agreement is within 2%). For these two days the transmission has its

ACPD
4, 7217–7279, 2004

lowest value. The tables show that the level of agreement (measured by, e.g. the mean difference) between measurement and model(s) is similar for CH_4 and for XCH_4. This shows that the time dependence of the quality of the retrieval is primarily determined by the channel 8 methane column retrieval and not by the channel 4 O_2 retrieval (as the division by O_2 performed to obtain XCH_4 does not change the time dependence). This time dependence needs further investigation by careful analysis of more data (e.g. using an entire year) which is beyond the scope of the current study but planned for the near future. Also its consequences for future versions of WFM-DOAS need to be assessed. Table 1 shows that N, the number of (latitude/longitude) grid boxes is significantly different for the four days investigated. This is mainly due to a significantly larger number of cloud free pixels over land for the northern hemisphere when going from northern hemisphere winter to northern hemisphere summer (see Fig. 18 with the corresponding KNMI/TM3 model data are shown in Fig. 18).

9.2. Carbon dioxide columns and XCO_2

In this section SCIAMACHY CO_2 measurements are compared with data from the MPI-BGC/TM3 global atmospheric transport model. Figure 20 shows the CO_2 columns as retrieved from the SCIAMACHY nadir measurements on 24 January 2003. The columns shown in Fig. 20 are those retrieved from cloud free pixels where a good or at least a reasonable fit of the WFM-DOAS model to the measurements has been achieved (fit error less than 10%, see also Sect. 9.1). Figure 21 shows the CO_2 columns of the MPI-BGC/TM3 model for the same day. The color scale is slighly different for both figures. Adjusting the color scale was necessary in order to better visualize the spatial column distributions in the two data sets. As can be seen, the spatial pattern are quite similar: both data sets show low columns over the Himalaya, the Andes and over south Africa and larger columns over north Africa and Australia. The linear correlation coefficient (Pearsons r) is 0.65, the mean difference is 0.16×10^{21} molecules/cm^2 (2.3%), and the standard deviation of the difference is $\pm0.50\times10^{21}$ molecules/cm^2 (7.7%).

ACPD
4, 7217–7279, 2004

Figures 23 and 24 show the corresponding CO_2 dry air column averaged mixing ratios XCO_2. The standard deviation of the difference is ±14.4 ppmv (3.9%) for the data over land. A prominent feature shown in Fig. 24 is an extended region of relatively low CO_2 mixing ratios in the southern part of Africa around Zambia. Here the mixing ratio is about 5 ppmv lower than typical values in the surroundings. The meteorology over southern Africa is dominated by a persistent high pressure system causing a large-scale, counterclockwise rotating closed circulation system. This acts as a giant containment reservoir for trace gases. The African tropical/sub-tropical regional sink in the model is primarily due to CO_2 uptake by vegetation in their main growing season. According to the model, this sink converts into a relatively strong source six months later, when the drought season begins.

Unfortunately, due to clouds, this apparently interesting region is not observed in the SCIAMACHY data on 24 January 2003 (see Fig. 23). In order to increase the number of cloud free pixels in this area all available orbits (seven days of SCIAMACHY data) from in the time period 24 January to 8 February 2003, have been processed. The results have been averaged (using only the cloud free pixels with a fit error less than 10%) and these averages are shown in Fig. 22 and 25. As can be seen, the spatial distribution of the CO_2 columns and mixing ratios as measured by SCIAMACHY over Africa show good agreement with the corresponding model data. The SCIAMACHY measurements (Fig. 25) show an extended region of low CO_2 mixing ratios over a similar region than the model. The measured CO_2 mixing ratios in the Zambia/Congo area are about 20 ppmv lower than typical values in its surroundings, whereas the depth of the CO_2 trough in the model is about 5 ppmv.

According to the model the air masses with the low CO_2 concentrations over Zambia are transported by winds westward over the Atlantic ocean where the mixing ratios in the latitude range 5° S–25° S are several ppmv lower than the background concentration (see Fig. 24). These air masses have been observed by ship-based solar occultation Fourier Transform Spectroscopy (FTS) measurements obtained in the same time period during a cruise of the German research vessel Polarstern (Warneke et al., sub-

mitted, 2004[1]). As shown in Fig. 26 the column averaged CO_2 mixing ratios measured by FTS in the latitude range 5° S–25° S are up to 5 ppmv lower than the background concentrations observed at higher and lower latitudes. This is roughly consistent with the model simulations. Figure 26 also shows that these extremely low CO_2 mixing ratios are not observed by the network of ground stations, which perform in situ measurements of the CO_2 mixing ratio at ground level.

In order to investigate the time behaviour of the retrieved CO_2 mixing ratios in this region more SCIAMACHY data have been processed. Figure 27 shows monthly averages of the CO_2 mixing ratios as measured by SCIAMACHY over Africa in the time period January to October 2003 (no consolidated orbit files for 2003 after October are currently available). The averages have been computed using all the consolidated orbit files that have been made available by ESA for this time period. The data shown are averages for three adjacent 5° latitude bands. Figure 27 shows that in January/February 2003 the measured mixing ratios are 5–20 ppmv lower that the January to October 2003 average. Six months later (July/August) the mixing ratios are 5–15 ppmv higher than the average. This time dependence is in reasonal agreement with the model results also shown in Fig. 27. The measured amplitude (~5–20 ppmv) is, however, significantly larger than the amplitude of the model data (~2–5 ppmv). The linear trend, wich is typically about 1.5 ppmv CO_2 increase per year, has not been subtracted from the data shown in Fig. 27. An accurate estimation of this trend from the data requires at least one full seasonal cycle, i.e. one year of data.

For the SCIAMACHY data a significant uncertainty is introduced by the large number of cloud contaminated pixels in the region around Zambia/Congo. Figure 25 shows large gaps indicating no cloud free pixels even in the several days average. The XCO_2 values observed for the cloud free pixels located in between the clouds are, however, consistent. They are consistenly lower than typical values in the surroundings. At

[1]Warneke, T., de Beek, R., Buchwitz, M., Notholt, J., Schulz, A., Velazco, V., and Schrems, O.: Shipborne solar absorption measurements of CO_2, CH_4, N_2O and CO and comparison with SCIAMACHY WFM-DOAS retrievals, Atmos. Chem. Phys. Discuss., submitted, 2004.

present we cannot entirely exclude that the measured trough of (very low) CO_2 mixing ratios over the Zambia/Congo area is at least partially due to the shielding effect of clouds not detected by the rather strict cloud identification algorithm used for this study.

In this context it is important to point out that errors on the retrieved (absolute) CO_2 columns (resulting from, e.g. clouds) are expected to cancel at least partially when the CO_2 mixing ratio is computed due to the division of the retrieved CO_2 columns by the simultaneously retrieved O_2 columns. This is nicely illustrated in Figs. 22 and 25 which show that most of the surface pressure induced effects (see, e.g. the extended regions of low CO_2 columns over Africa visible in Figs. 21 and 22) are not present in the XCO_2 field (see Figs. 24 and 25) where only a nearly circular region of low mixing ratios in the area around Zambia/Congo is visible.

Figure 28 shows similar results as Fig. 27 but for global data (over land), i.e. not restricted to Africa, and for an extended latitude range. In the latitude range 10° S–25° S (shown in red) the seasonal behaviour of the global average is similar as the average over Africa shown in Fig. 27. The amplitude, however, is somewhat lower due to the smoothing introduced by including obserations over land areas where (according to the model, see Fig. 24) the column averaged mixing ratios are closer to the background concentration, i.e. where the surface fluxes do not result in large regional mixing ratio variations as over Zambia/Congo. For northern latitudes Fig. 28 shows a similar seasonal behaviour as in the southern hemisphere but with the expected six-months phase shift. Figure 29 shows the corresponding results of the MPI-BGC/TM3 model. Apart from the different amplitude (which is about a factor of four higher in the SCIAMACHY data) the agreement between measurement and model is good in the latitude range 10° S–25° S (shown in red). Outside this latitude band the differences are larger. For example in the northern mid-latitudes the maximum is around April/May in the model data but around February in the SCIAMACHY data.

Figure 28 may be compared with a similarly structured figure from Chedin et al. (2003), where monthly averaged mid-tropospheric CO_2 mixing ratios are shown derived from four years of TOVS/NOAA-10 data in the latitude range 20° S–20° N. Fig-

ACPD
4, 7217–7279, 2004

ure 2 of Chedin et al. (2003) shows similarities with the results shown in Figs. 28 and 29 but also differences. In the latitude range 0°–20° N, for example, the mixing ratios shown in Chedin et al. (2003) are in reasonable agreement with the model data shown in Fig. 29. The seasonal cycles are similar but the amplitudes are different (e.g., 20° N–15° N: Chedin: 3–4 ppmb, MPI-BGC model: 1–2 ppmv). In the latitude range 0°–20° S, however, the mixing ratios shown in Chedin et al. (2003) significantly differ from the mixing ratios shown in Fig. 28 and 29. For example, the most pronounced mixing ratio minima are in July-September in Chedin et al. (2003) whereas these are the month where the largest mixing ratios have been measured by SCIAMACHY.

10. Conclusions

SCIAMACHY nadir spectra recorded in the time period January to October 2003 have been processed with version 0.4 of the WFM-DOAS inversion algorithm to retrieve vertical columns of CH_4, CO_2, and O_2. The O_2 columns have been used to compute O_2 or air normalized greenhouse gas columns, the so called dry air column averaged mixing ratios XCH_4 and XCO_2. It has been shown that for cloud free measurements over land the SCIAMACHY data are in reasonable agreement with global models of transport and chemistry.

For methane four days have been analysed in detail. The inter-hemispheric difference of the methane mixing ratio as determined from single day cloud free measurements over land is in the range 30–110 ppbv and in good agreement with the corresponding model data which are in the range 48–71 ppbv. The mean differences between the measured and the modelled absolute columns (in molecules/cm^2) are +0.5% and +1.8% for two of the analysed days but −9.3% and −15.3% for the two other days. This indicates that there is a time dependent bias. This bias is most probably related to time dependent instrument characteristics (due to ice build up on the detectors) that have not yet been considered good enough in the calibration and/or retrieval process. More data need to be analysed to confirm this. The standard deviation

ACPD
4, 7217–7279, 2004

of the difference is less than 0.4×10^{19} molecules/cm^2 (~10%) for all four days. The linear correlation coefficient r is in the range 0.55–0.88.

The CO_2 measurements also agree with the model data within a few percent. The CO_2 measurements of SCIAMACHY show that for the first time a natural CO_2 source/sink region has been detected using satellite measurements.

In spite of the encouraging results presented here, there is room and need for further improvements. For example, only small spectral windows have been analysed so far covering only a few of the methane and carbon dioxide absorption lines detected by SCIAMACHY. In this context it will be very interesting to retrieve methane (also) from SCIAMACHY channel 6 not affected by ice-layer build up as channel 8 which has been used for this study. Our ultimate goal is to obtain nearly bias free retrievals with a single measurement precision close to the theoretical limit of ~1% (Buchwitz et al., 2000a).

Acknowledgements. We thank G. C. Toon, JPL/NASA, for helpful discussions related to Fig. 1, S. Noël and K. Bramstedt for assistance in pre-processing the SCIAMACHY spectra, M. Eisinger for the source code of the DOAS fitting software "kvant", and M. Krol for coordination of the TM5 model development. We also acknowledge European Commission (EC) 6th Framework Programme (FP) Network of Excellence ACCENT for exchange of useful information and the German computer system Hochleistungsrechner Nord (HLRN). Thanks also to RIVM/TNO (Dutch National Institute for Public Health and the Environment) for their EDGAR 3.2 database (Olivier, 2002), and to C. Le Quéré and K. Trusilova for providing CO_2 flux data. NCEP reanalysis 2 data were provided by the NOAA-CIRES Climate Diagnostics Center, Boulder, Colorado, USA, from their web site at http://www.cdc.noaa.gov. Funding for this study came from the EC (5th FP on Energy, Environment and Sustainable Development, Contract no. EVG1-CT-2002-00079, project EVERGREEN). The University of Bremen contribution has been funded in addition by the German Ministry for Research and Education (BMBF) via DLR-Bonn (Grants 50EE0027 and 50EE9901) and GSF/PT-UKF (Grant 07UFE12/8), and by the University and the State of Bremen.

References

Andreae, M. and Merlet, P.: Emission of trace gases and aerosols from biomass burning, Global Biogeochem. Cycles, 15, 955–966, 2001. 7236

Bergamaschi, P., Krol, M., Dentener, F., Vermeulen, A., Meinhardt, F., Graul, R., Peters, W., and Dlugokencky, E. J.: Inverse modelling of national and European CH_4 emissions using the atmospheric zoom model TM5, Atmos. Chem. Phys. Discuss., accepted, 2004. 7233, 7236

Bovensmann, H., Burrows, J. P., Buchwitz, M., Frerick, J., Noël, S., Rozanov, V. V., Chance, K. V., and Goede, A.: SCIAMACHY – Mission Objectives and Measurement Modes, J. Atmos. Sci., 56, 127–150, 1999. 7222, 7230

Bovensmann, H., Buchwitz, M., Frerick, J., Hoogeveen, R., Kleipool, Q., Lichtenberg, G., Noël, S., Richter, A., Rozanov, A., Rozanov, V. V., Skupin, J., von Savigny, C., Wuttke, M., and Burrows, J. P.: SCIAMACHY on ENVISAT: In-flight optical performance and first results, in Remote Sensing of Clouds and the Atmosphere VIII, edited by Schäfer, K. P., Comèron, A., Carleer, M. R., and Picard, R. H., vol. 5235 of Proceedings of SPIE, 160–173, 2004. 7222, 7223

Buchwitz, M. and Burrows, J. P.: Retrieval of CH_4, CO, and CO_2 total column amounts from SCIAMACHY near-infrared nadir spectra: Retrieval algorithm and first results, in Remote Sensing of Clouds and the Atmosphere VIII, edited by Schäfer, K. P., Comèron, A., Carleer, M. R., and Picard, R. H., vol. 5235 of Proceedings of SPIE, 375–388, 2004. 7224, 7226, 7251, 7255

Buchwitz, M., Rozanov, V. V., and Burrows, J. P.: A near infrared optimized DOAS method for the fast global retrieval of atmospheric CH_4, CO, CO_2, H_2O, and N_2O total column amounts from SCIAMACHY/ENVISAT-1 nadir radiances, J. Geophys. Res., 105, 15 231–15 246, 2000a. 7224, 7226, 7244

Buchwitz, M., Rozanov, V. V., and Burrows, J. P.: A correlated-k distribution scheme for overlapping gases suitable for retrieval of atmospheric constituents from moderate resolution radiance measurements in the visible/near-infrared spectral region, J. Geophys. Res., 105, 15 247–15 262, 2000b. 7225

Buchwitz, M., de Beek, R., Bramstedt, K., Noël, S., Bovensmann, H., and Burrows, J. P.: Global carbon monoxide as retrieved from SCIAMACHY by WFM-DOAS, Atmos. Chem. Phys. Discuss., 4, 2805–2837, 2004, SRef-ID: 1680-7375/acpd/2004-4-2805. 7224

Burrows, J. P., Hölzle, E., Goede, A. P. H., Visser, H., and Fricke, W.: SCIAMACHY – Scanning Imaging Absorption Spectrometer for Atmospheric Chartography, Acta Astronautica, 35(7), 445–451, 1995. 7222

Chedin, A., Serrar, S., Scott, N. A., Crevoisier, C., and Armante, R.: First global measurement of midtropospheric CO_2 from NOAA polar satellites: Tropical zone, J. Geophys. Res., 108 (D18), 4581, doi:10.1029/2003JD003439, 2003. 7220, 7242, 7243

Clerbaux, C., Hadji-Lazaro, J., Turquety, S., Megie, G., and Coheur, P.-F.: Trace gas measurements from infrared satellite for chemistry and climate applications, Atmos. Chem. Phys., 3, 1495–1508, 2003, SRef-ID: 1680-7324/acp/2003-3-1495. 7220

Coldewey-Egbers, M., Weber, M., Buchwitz, M., and Burrows, J. P.: Application of a modified DOAS method for total ozone retrieval from GOME data at high polar latitudes, Adv. Space Res., 34, 749–753, 2004. 7224

Connor, B., Kuang, Z., Toon, G., Crisp, D., Wood, S., Barnet, C., and Buchwitz, M.: The averaging kernel of CO_2 column measurements by the Orbiting Carbon Observatory (OCO), its use in inverse modeling, and comparison to AIRS, SCIAMACHY, and ground-based FTIR, Poster presented at the AGU Fall Meeting (available from http://www.iup.physik.uni-bremen.de/sciamachy/NIR_NADIR_WFM_DOAS/), 2003. 7229

Goody, R. M. and Yung, Y. L.: Atmospheric Radiation, Oxford University Press, New York, 1989. 7229

Gurney, K. R., Law, R. M., Denning, A. S., Rayner, P. J., Baker, D., Bousquet, P., Bruhwiler, L., Chen, Y.-H., Ciais, P., Fan, S., Fung, I. Y., Gloor, M., Heimann, M., Higuchi, K., John, J., Maki, T., Maksyutov, S., Masarie, K., Peylin, P., Prather, M., Pak, B. C., Randerson, J., Sarmiento, J., Taguchi, S., Takahashi, T., and Yuen, C.-W.: Towards robust regional estimates of CO_2 sources and sinks using atmospheric transport models, Nature, 415, 626–629, 2002. 7219

Heimann, M. and Körner, S.: The Global Atmospheric Tracer Model TM3, Model Description and Users Manual Release 3.8a, Tech. Rep. 5, Max Planck Institute for Biogeochemistry (MPI-BGC), Jena, Germany, 2003. 7233

Houweling, S., Kaminski, T., Dentener, F., Lelieveld, J., and Heimann, M.: Inverse modeling of methane sources and sinks using the adjoint of a global transport model, J. Geophys. Res., 105 (D21), 26 137–26 160, 1999. 7219, 7232

Houweling, S., Breon, F.-M., Aben, I., Rödenbeck, C., Gloor, M., Heimann, M., and Ciais, P.: Inverse modeling of CO_2 sources and sinks using satellite data: A synthetic inter-comparison of measurement techniques and their performance as a function of space and time, Atmos.

ACPD
4, 7217–7279, 2004

Chem. Phys., 4, 523–538, 2003, SRef-ID: 1680-7324/acp/2004-4-523. 7220
Kleipool, Q.: SCIAMACHY: Recalculation of OPTEC5 Non-Linearity, Tech. Rep. SRON-SCIA-PhE-RP-013, available from the author (Q.L.Kleipool@sron.nl), SRON, Utrecht, The Netherlands, 2003. 7223
Kobayashi, H., Shimota, A., Kondo, K., Okumura, E., Kameda, Y., Shimoda, H., and Ogawa, T.: Development and evaluation of the Interferometric Monitor for Greenhouse Gases: a high throughput Fourier transform infrared radiometer for nadir Earth observations, Appl. Opt., 38, 6801–6807, 1999a. 7220
Kobayashi, H., Shimota, A., Yoshigahara, C., Yoshida, I., Uehara, Y., and Kondo, K.: Satellite-borne high-resolution FTIR for lower atmosphere sounding and its evaluation, IEEE Transactions on Geoscience and Remote Sensing, 37 (3), 1496–1507, 1999b. 7220
Krol, M. C., Houweling, S., Bregman, B., van den Broek, M., Segers, A., van Velthoven, P., Peters, W., Dentener, F., and Bergamaschi, P.: The two-way nested global chemistry-transport zoom model TM5: Algorithm and applications, Atmos. Chem. Phys. Discuss., 3975–4018, 2004. 7233
Lelieveld, J. and Dentener, F. J.: What controls tropospheric ozone?, J. Geophys. Res., 105, 3531–3551, 2000. 7232
Muller, J.-F. and Brasseur, G.: IMAGES: A three-dimensional chemical transport model of the global troposphere, J. Geophys. Res., 100, 16 445–16 490, 1995. 7233
Noël, S., Buchwitz, M., and Burrows, J. P.: First retrieval of global water vapour column amounts from SCIAMACHY measurements, Atmos. Chem. Phys., 4, 111–125, 2004. 7224
Olivier, J. G. J.: Greenhouse gas emissions: 1. Shares and trends in greenhouse gas emissions; 2. Sources and Methods; Greenhouse gas emissions for 1990 and 1995, in CO_2 emissions from fuel combustion 1971–2000, ISBN 92-64-09794-5, pp. III.1–III.31, International Energy Agency (IEA), Paris, 2002 edn., 2002. 7244
Press, W., Teukolsky, S., Vetterling, W., and Flannery, B.: Numerical Recipes in Fortran, Cambridge University Press, London, 1992. 7225
Rayner, P. J. and O'Brian, D. M.: The utility of remotely sensed CO_2 concentration data in surface inversions, Geophys. Res. Lett., 28, 175–178, 2001. 7219
Rothman, L. S., Barbe, A., Benner, D. C., Brown, L. R., Camy-Peyret, C., Carleer, M. R., Chance, K., Clerbaux, C., Dana, V., Devi, V. M., Fayt, A., Flaud, J. M., Gamache, R. R., Goldman, A., Jacquemart, D., Jucks, K. W., Lafferty, W. J., Mandin, J. Y., Massie, S. T., Nemtchinov, V., Newnham, D. A., Perrin, A., Rinsland, C. P., Schroeder, J., Smith, K. M.,

Smith, M. A. H., Tang, K., Toth, R. A., Vander Auwera, J., Varanasi, P., and Yoshino, K.: The HITRAN molecular spectroscopic database: edition of 2000 including updates through 2001, J. Quant. Spectrosc. Radiat. Transfer, 82, 5–44, 2003. 7231

Takahashi, T., Sutherland, S. C., Sweeney, C., Poisson, A., Metzl, N., Tilbrook, B., Bates, N., Wanninkhof, R., Feely, R. A., Sabine, C., Olafsson, J., and Nojiri, Y.: Global sea-air CO_2 flux based on climatological surface ocean pCO_2, and seasonal biological and temperature effects, Deep-Sea Research, 49, 1601–1622, 2002. 7234

Yang, Z. H., Toon, G. C., Margolis, J. S., and Wennberg, P. O.: Ground based inversion of CO_2 column densities from solar spectra, Geophys. Res. Lett., 29, doi:10.1029/2001GL014537, 2002. 7232

Table 1. Overview of the comparison of the CH_4 columns as retrieved from SCIAMACHY for cloud free scenes over land for four days with CH_4 KNMI/TM3 model columns. The last column lists the average transmission of SCIAMACHY channel 8 relative to first in-orbit measurements (Source: SCIAMACHY Operations Support Team web page: http://atmos.af.op.dlr.de/projects/scops/).

Model	Day	N grid boxes	Pearsons r CH_4 col.	Mean difference SCIA-model (10^{19} molecules/cm^2)	Standard deviation SCIA-model (10^{19} molecules/cm^2)	Channel 8 relative transmission [-]
KNMI/TM3	2003/01/24	2770	0.88	+0.06 (+1.8%)	0.18 (5.7%)	0.9
	2003/03/28	4437	0.82	−0.32 (−9.3%)	0.21 (6.5%)	0.7
	2003/05/30	7581	0.55	+0.02 (+0.5%)	0.38 (11.0%)	0.8
	2003/07/23	8535	0.62	−0.53 (−15.3%)	0.32 (8.9%)	0.6

ACPD
4, 7217–7279, 2004

Table 2. Overview of the comparison of XCH_4 as retrieved from SCIAMACHY for cloud free scenes over land for four days with XCH_4 KNMI/TM3 and JRC/TM5 model values. The latitudes listed in the table are the latitudes chosen to separate the northern from the southern hemisphere taking into account the position on the inner tropical concergence zone (ITCZ) for the calculation of the inter-hemispheric difference (IHD) of the column averaged methane mixing ratio XCH_4.

Model	Day	Mean XCH_4 SCIA (ppbv)	Mean XCH_4 model (ppbv)	Latitude (deg)	IHD SCIA (ppbv)	IHD model (ppbv)	Mean difference SCIA-model (ppbv)	Standard deviation (ppbv)	Pearsons r XCH_4
KNMI/ TM3	2003/01/24	1752	1737	−10	53	71	+15 (+0.9%)	98 (5.7%)	0.19
	2003/03/28	1564	1747	0	30	55	−183 (−10.5%)	89 (5.1%)	0.10
	2003/05/30	1805	1754	3	110	56	+51 (+2.9%)	200 (11.3%)	0.25
	2003/07/23	1498	1758	15	31	60	−260 (−14.8%)	121 (6.8%)	0.04
JRC/ TM5	2003/01/24	1752	1742	−10	53	56	+10 (+0.6%)	97 (5.6%)	0.18
	2003/03/28	1564	1750	0	30	48	−186 (−10.6%)	89 (5.1%)	0.07
	2003/05/30	1805	1756	3	110	56	+48 (+2.7%)	200 (11.3%)	0.25
	2003/07/23	1498	1764	15	31	63	−266 (−15.1%)	122 (6.8%)	0.01

ACPD
4, 7217–7279, 2004

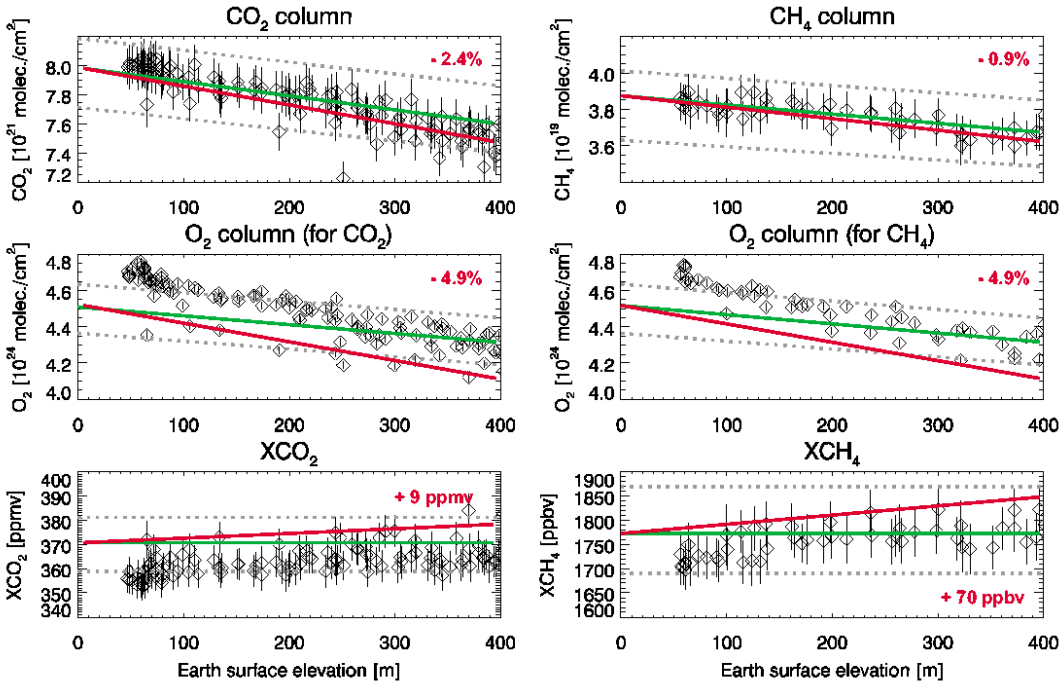

Fig. 1. Correlation of the CO_2, CH_4, and O_2 columns as retrieved from SCIAMACHY with surface elevation from measurements around Senegal on 23 January 2003. The black symbols are the retrieved columns and the black vertical lines are the fit errors (see Sect. 4). The green lines show the expected values for the columns computed using a standard pressure profile. The dotted lines indicate their estimated variability (±3% for CO_2 and O_2, ±5% for CH_4). The red lines have been determined from simulated retrievals (see main text for details). The numbers given at the right hand side of each panel show the column retrieval error for 400 m surface elevation as determined from simulated retrievals (figure adapted from Buchwitz and Burrows, 2004).

ACPD
4, 7217–7279, 2004

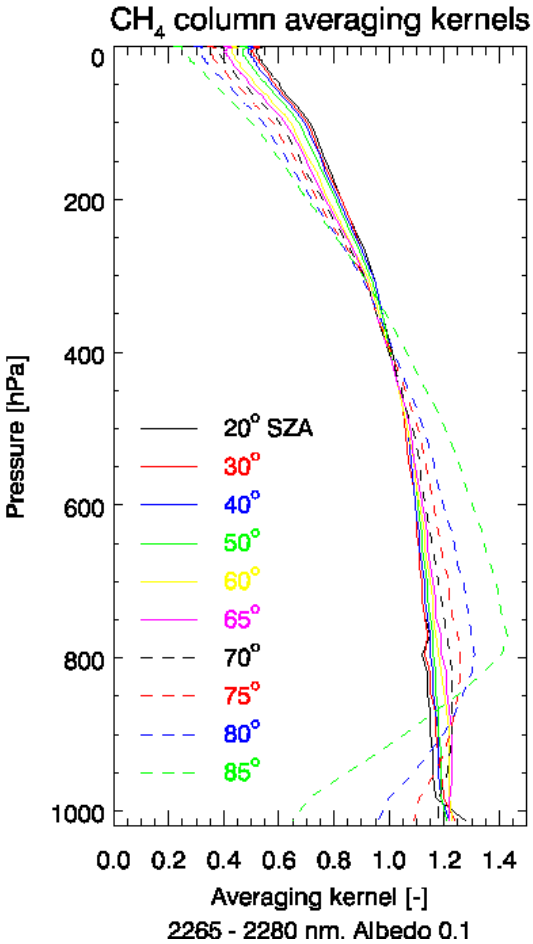

Fig. 2. SCIAMACHY CH_4 column averaging kernels computed by applying WFM-DOAS to simulated spectra for various solar zenith angles.

ACPD
4, 7217–7279, 2004

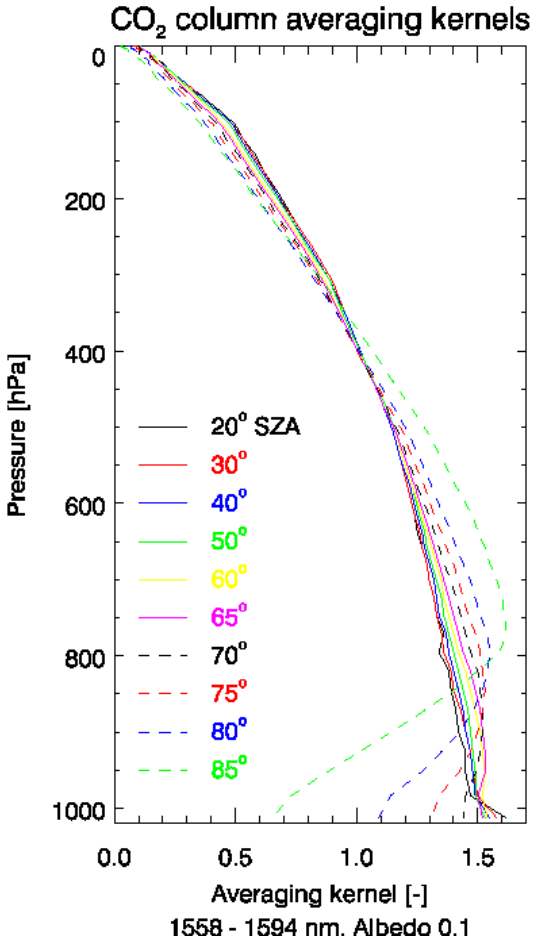

Fig. 3. As Fig. 2 but for CO_2.

ACPD
4, 7217–7279, 2004

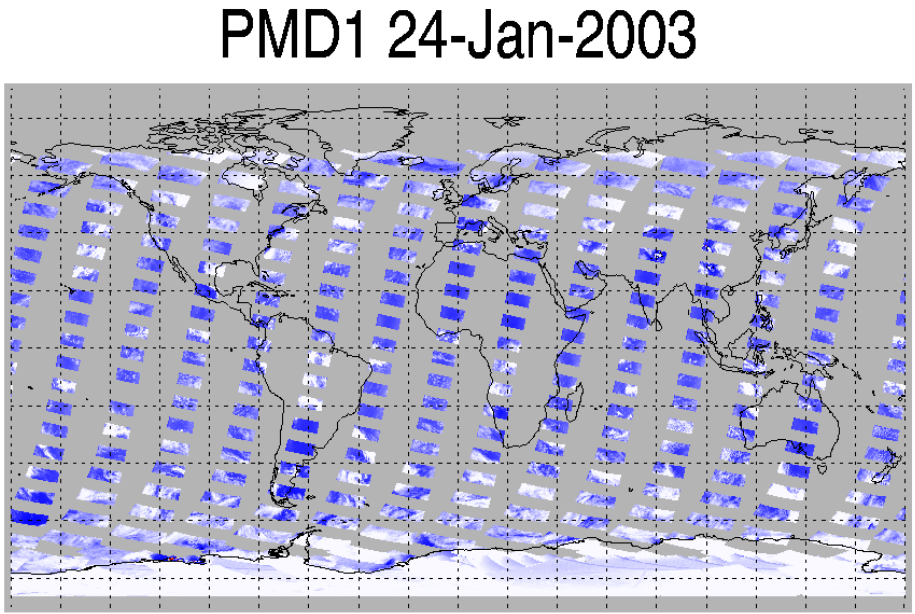

Fig. 4. Map of SCIAMACHY PMD 1 nadir reflectivity for 24 January 2003; color code: white corresponds to high PMD signal (e.g. due to clouds), blue to low signal (cloud free).

ACPD

4, 7217–7279, 2004

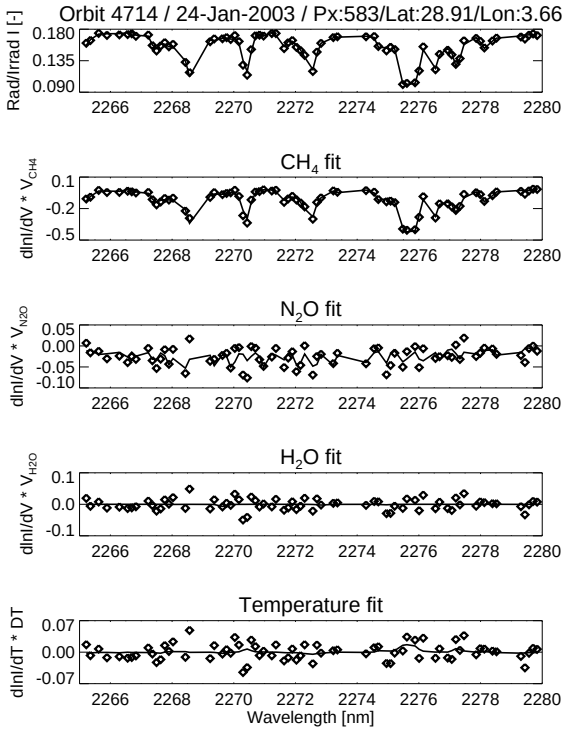

Fig. 5. Typical example of a WFM-DOAS fit in the spectral region used for methane retrieval. SCIAMACHY sun-normalized nadir spectrum (symbols) and WFM-DOAS model spectrum (solid line) is shown in the top panel. The other panels show the fit results for the individual fit parameters, e.g. methane (second panel). The retrieved methane column is 3.59×10^{19} molecules/cm^2 ±3%. In addition to methane, N_2O and H_2O (both are weak absorbers in this spectral region) and a shift of the temperature profile are included in the fit (see Buchwitz and Burrows, 2004, for details). The retrieved N_2O column is 6.2×10^{18} molecules/cm^2 ±22%. The root-mean-square (RMS) difference between measurement and WFM-DOAS model is 0.017 (1.7%).

ACPD
4, 7217–7279, 2004

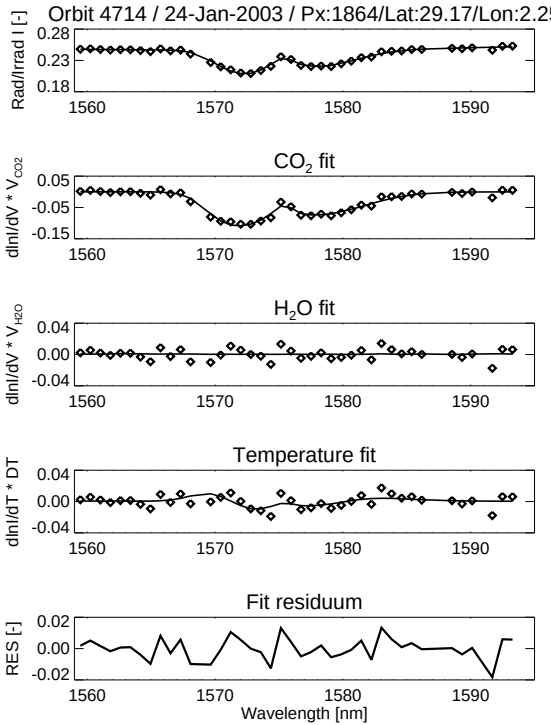

Fig. 6. As Fig. 5 but for CO_2. The retrieved CO_2 column is 8.11×10^{21} molecules/cm^2 ±6%. The root-mean-square (RMS) difference between measurement and WFM-DOAS model is 0.0066 (0.66%).

ACPD
4, 7217–7279, 2004

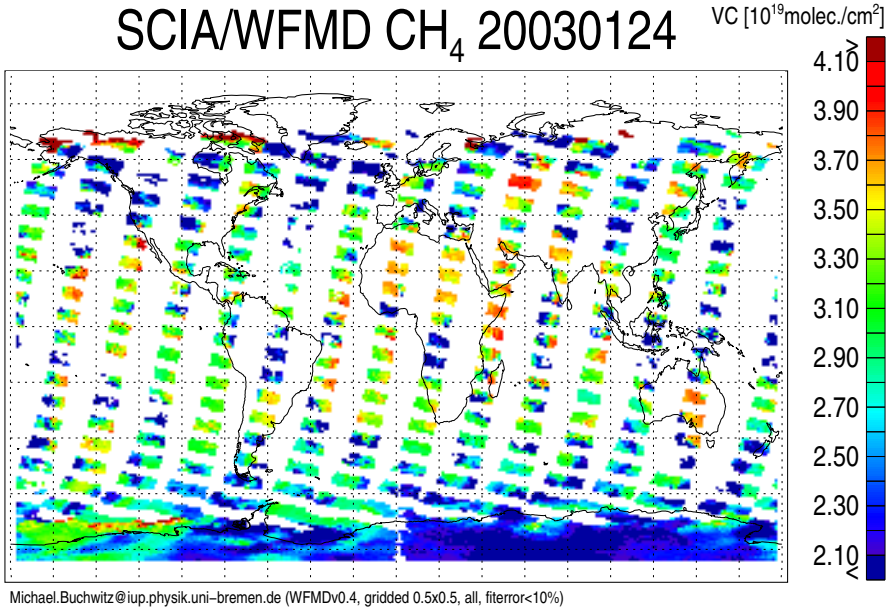

Fig. 7. Methane vertical columns (VC) on 24 January 2003, as retrieved from SCIAMACHY. Shown are all data with fit errors less than 10%.

ACPD
4, 7217–7279, 2004

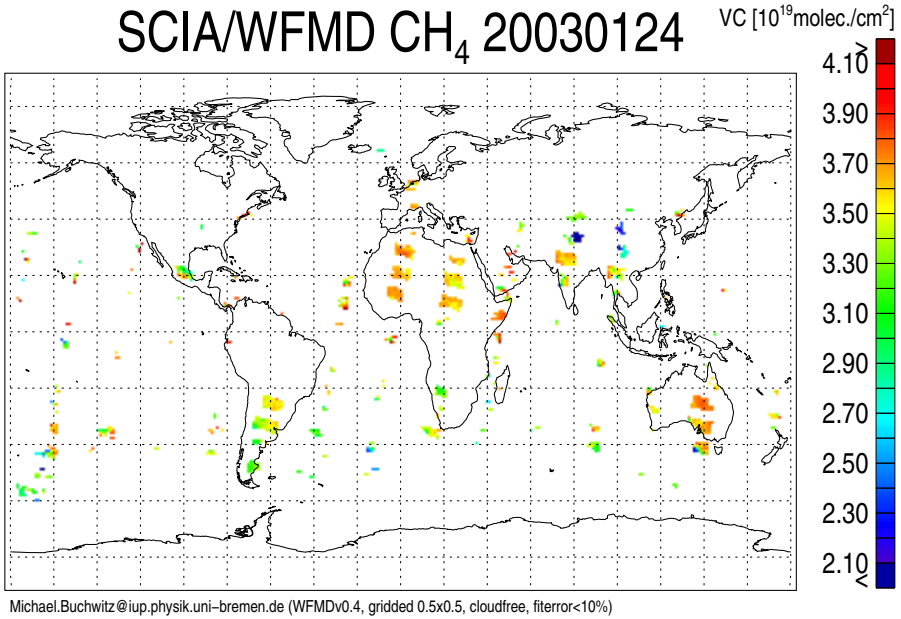

Fig. 8. As Fig. 7 but only for strictly cloud free pixels.

ACPD
4, 7217–7279, 2004

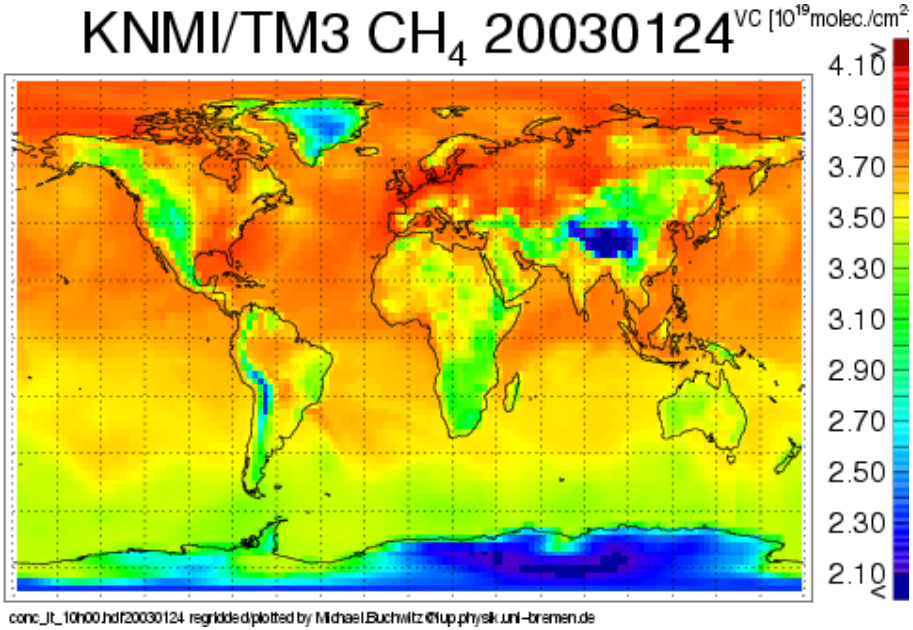

Fig. 9. Methane vertical columns from KNMI/TM3 model for 24 January 2003.

ACPD
4, 7217–7279, 2004

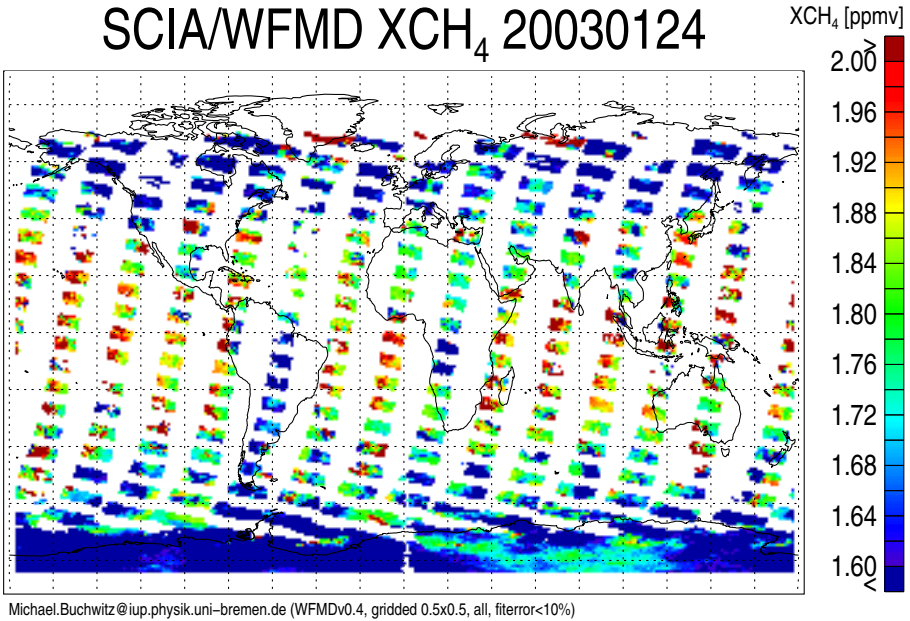

Fig. 10. XCH_4 from 24 January 2003, as retrieved from SCIAMACHY. Shown are all data with fit errors less than 10%.

ACPD
4, 7217–7279, 2004

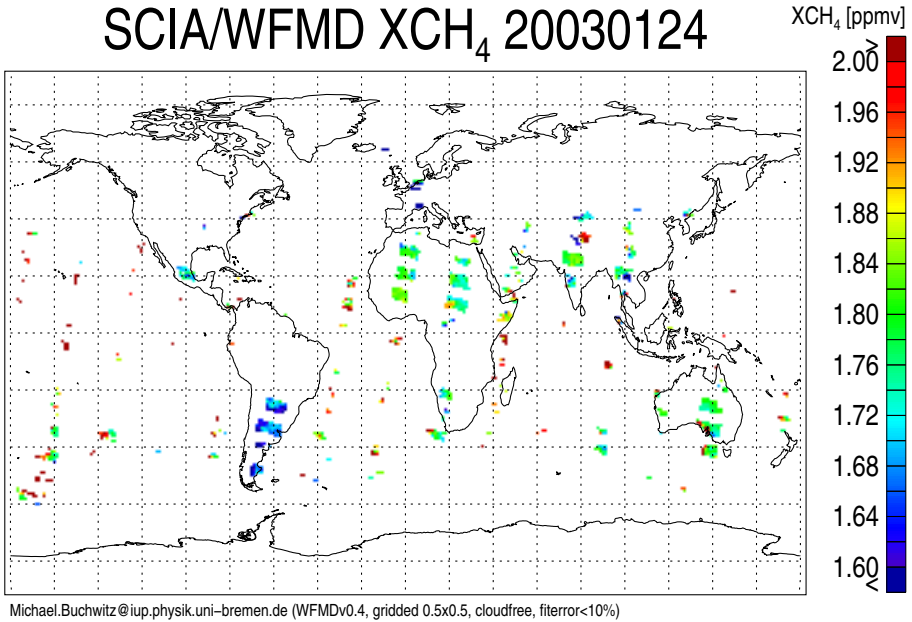

Fig. 11. As Fig. 10 but only for strictly cloud free pixels.

ACPD
4, 7217–7279, 2004

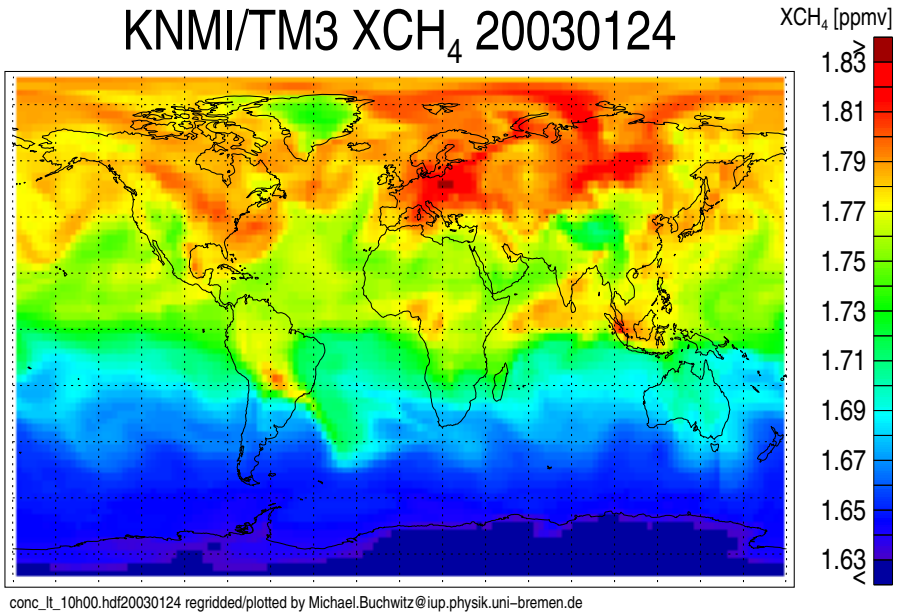

Fig. 12. XCH_4 from KNMI/TM3 model for 24 January 2003.

ACPD
4, 7217–7279, 2004

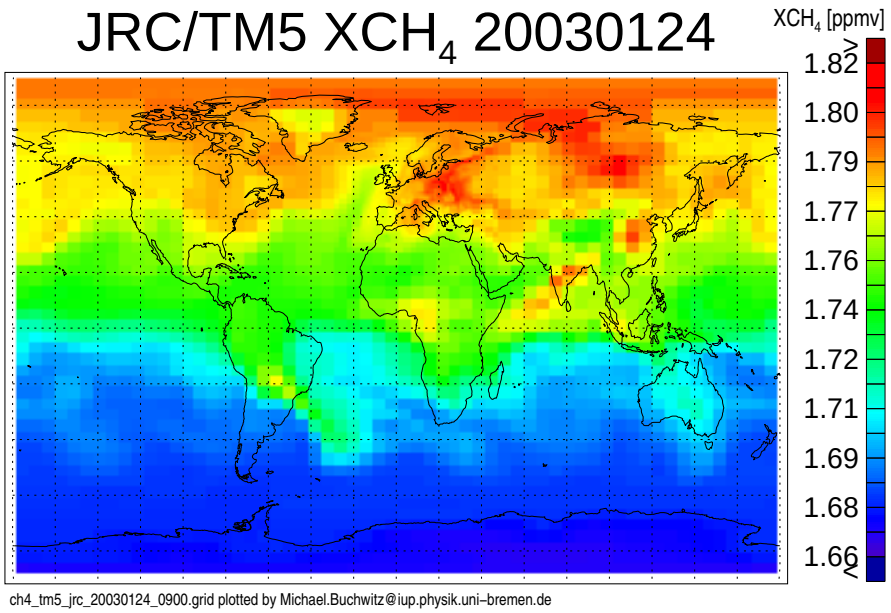

Fig. 13. As Fig. 12 but for the TM5 model of JRC.

ACPD
4, 7217–7279, 2004

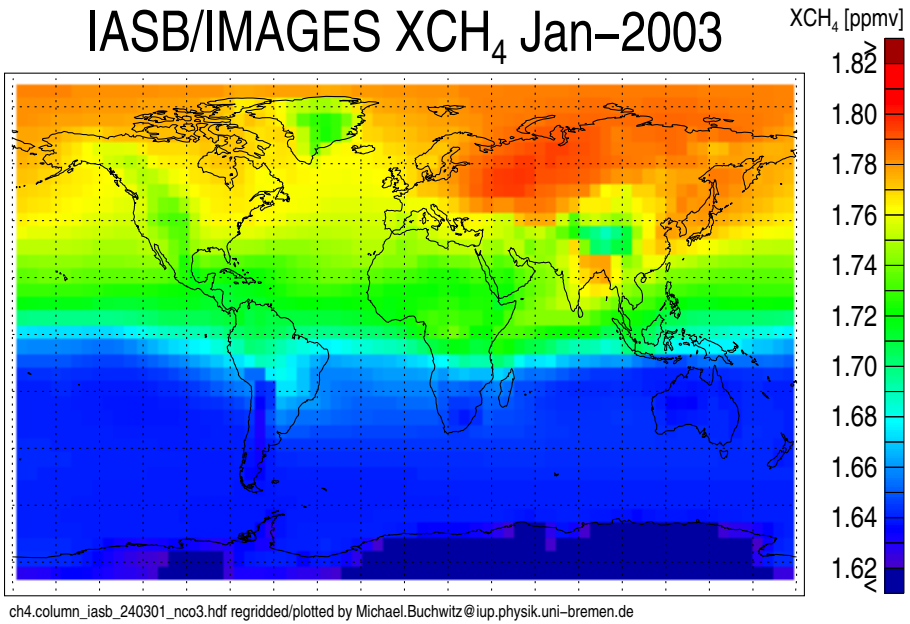

Fig. 14. As Fig. 12 but for the IMAGES model of IASB. Here, the monthly mean XCH_4 field is shown for January 2003.

ACPD
4, 7217–7279, 2004

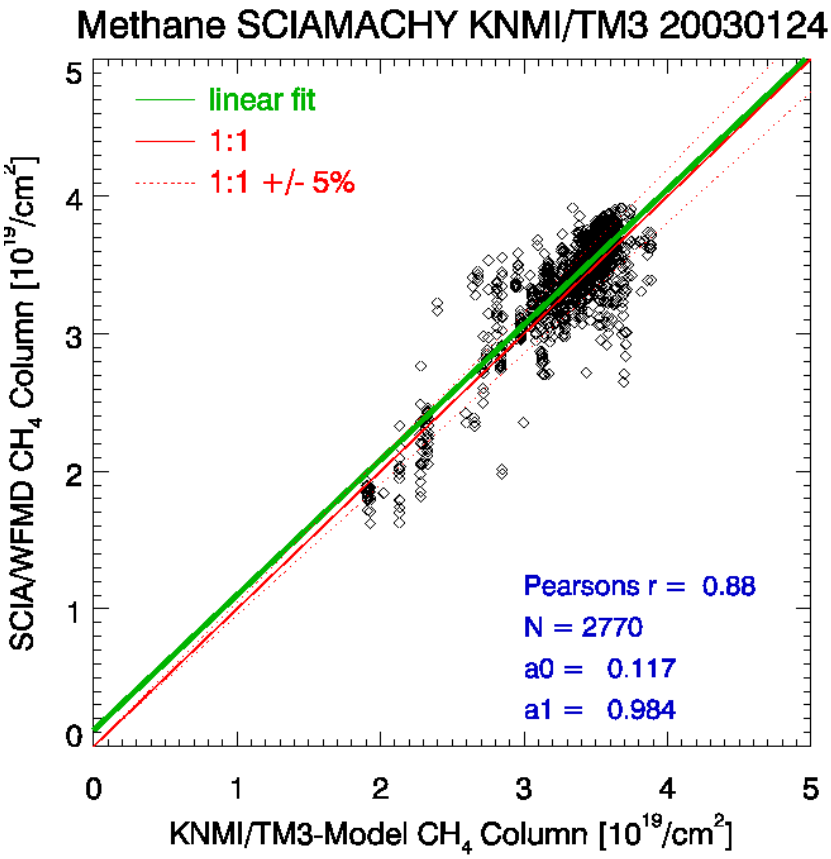

Fig. 15. Correlation of the SCIAMACHY CH_4 column measurements shown in Fig. 8 with the corresponding KNMI/TM3 model data shown in Fig. 9. The comparison is limited to measurements over land. The linear correlation coefficient r is 0.88. The number of data points N is 2770. The offset and slope parameters of the linear fit are a_0=0.12 and a_1=0.98.

ACPD
4, 7217–7279, 2004

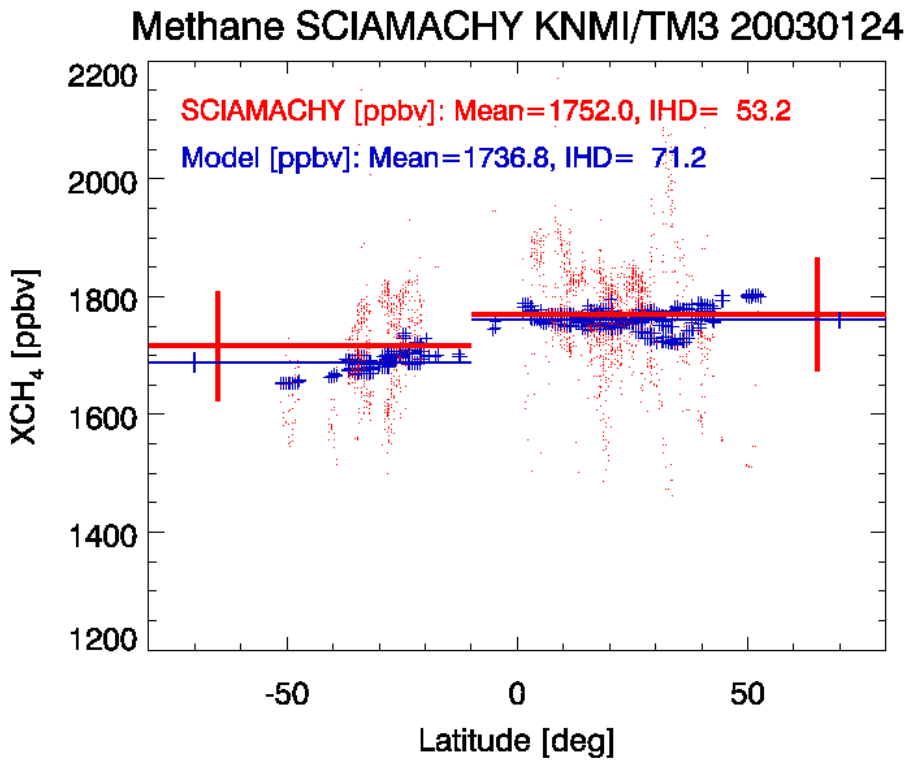

Fig. 16. XCH_4 as a function of latitude as measured by SCIAMACHY (shown as red points; see also Fig. 11) and the corresponding KNMI/TM3 model data (blue crosses). The two horizontal red lines show the average values of the SCIAMACHY data in the latitude bands −90 to −10° and −10 to +90°. The two vertical red lines indicate the standard deviation of the SCIAMACHY data in the two latitude bands. The blue lines show the same quantities but for the KNMI/TM3 model. The comparison is limited to cloud free measurements over land. The mean value of all the SCIAMACHY data is 1752 ppbv and the corresponding model value is 1737 ppbv. The inter-hemispheric difference (IHD) as measured by SCIAMACHY is 53 ppbv and the corresponding model value is 71 ppbv.

ACPD
4, 7217–7279, 2004

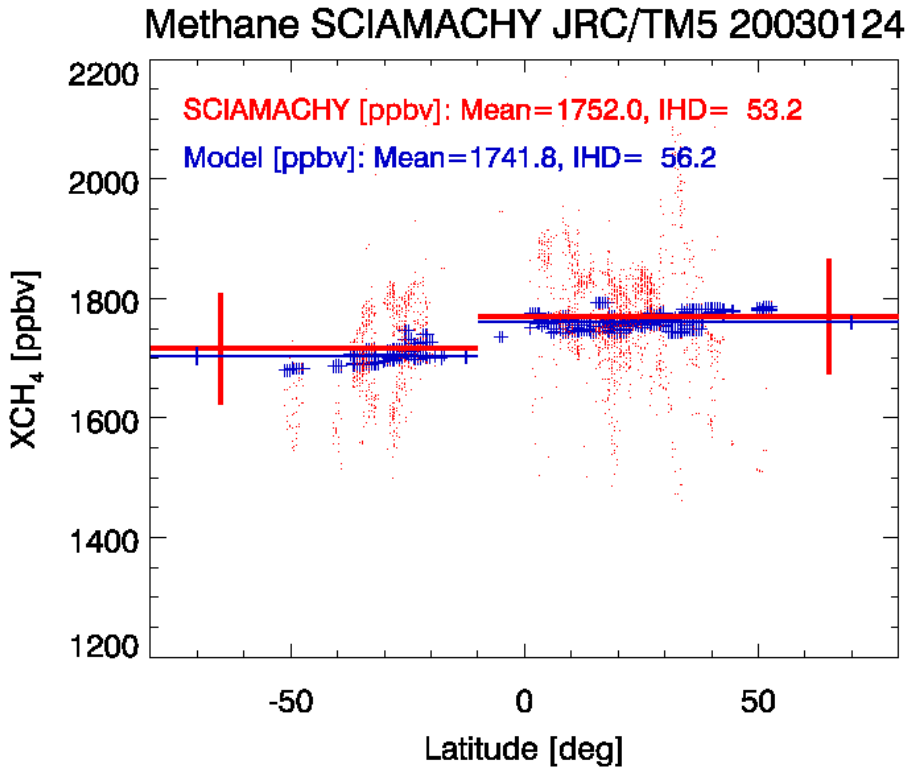

Fig. 17. As Fig. 16 but for the TM5 model of JRC.

ACPD
4, 7217–7279, 2004

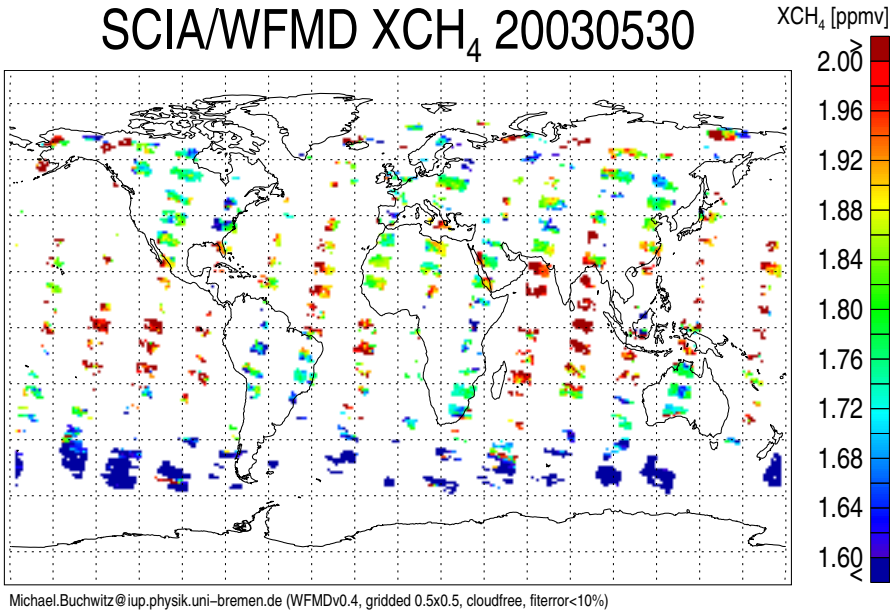

Fig. 18. As Fig. 11 but for 30 May 2003.

ACPD
4, 7217–7279, 2004

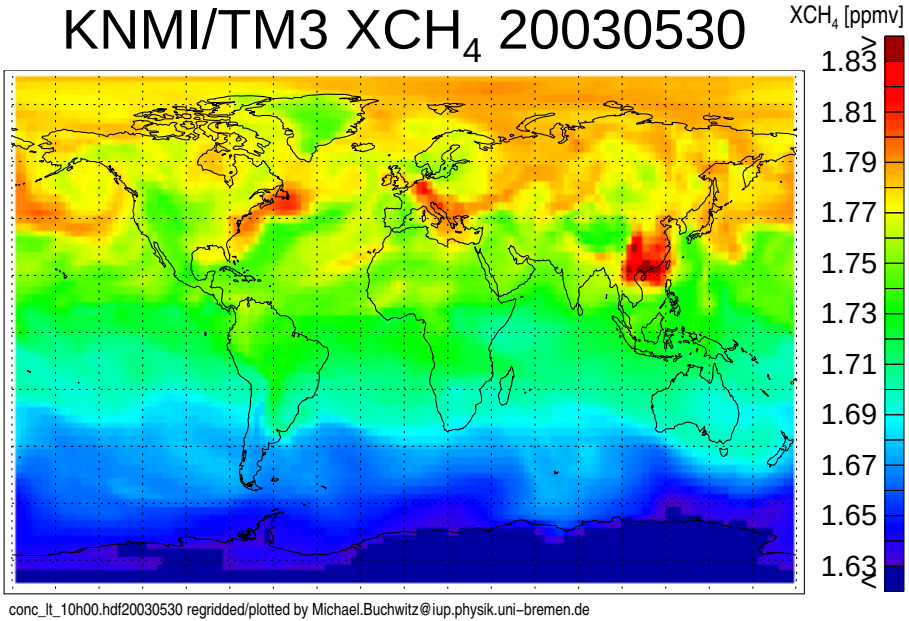

Fig. 19. XCH_4 from KNMI/TM3 model for 30 May 2003.

ACPD
4, 7217–7279, 2004

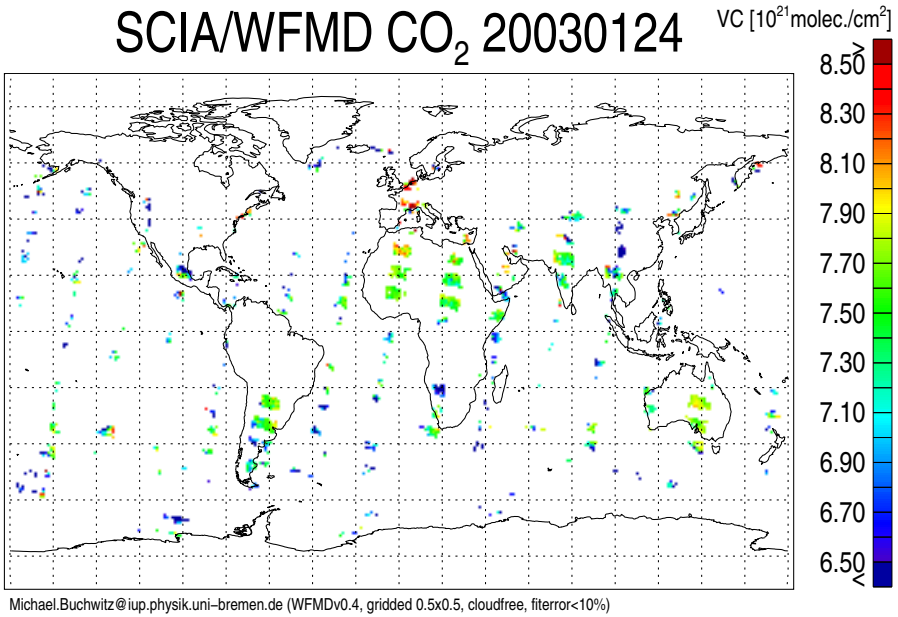

Fig. 20. CO_2 columns for cloud free scenes as retrieved from SCIAMACHY. Shown are only the columns for strictly cloud free pixels with a fit error less than 10%.

ACPD
4, 7217–7279, 2004

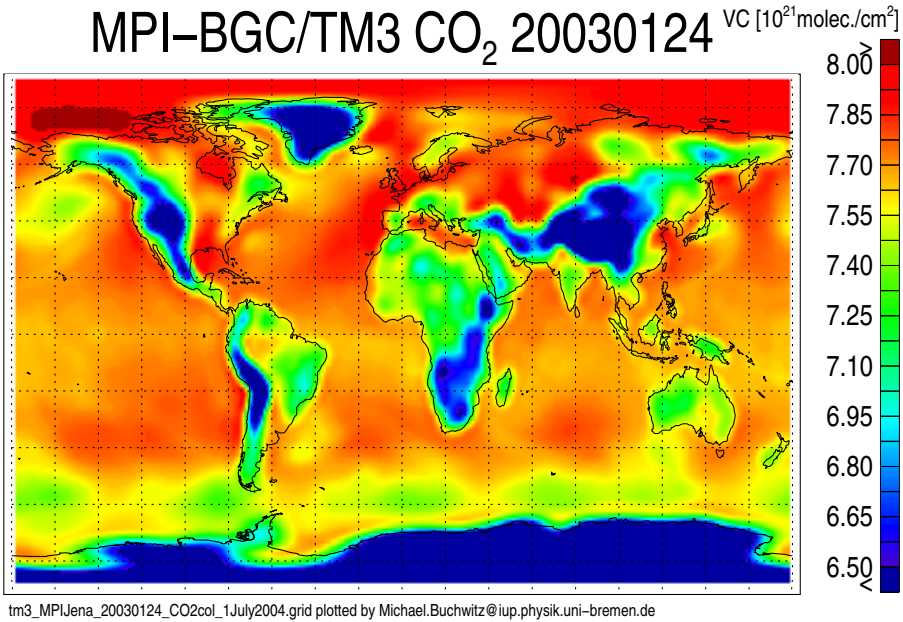

Fig. 21. CO_2 vertical columns (VC) from the TM3 model of MPI-BGC.

ACPD
4, 7217–7279, 2004

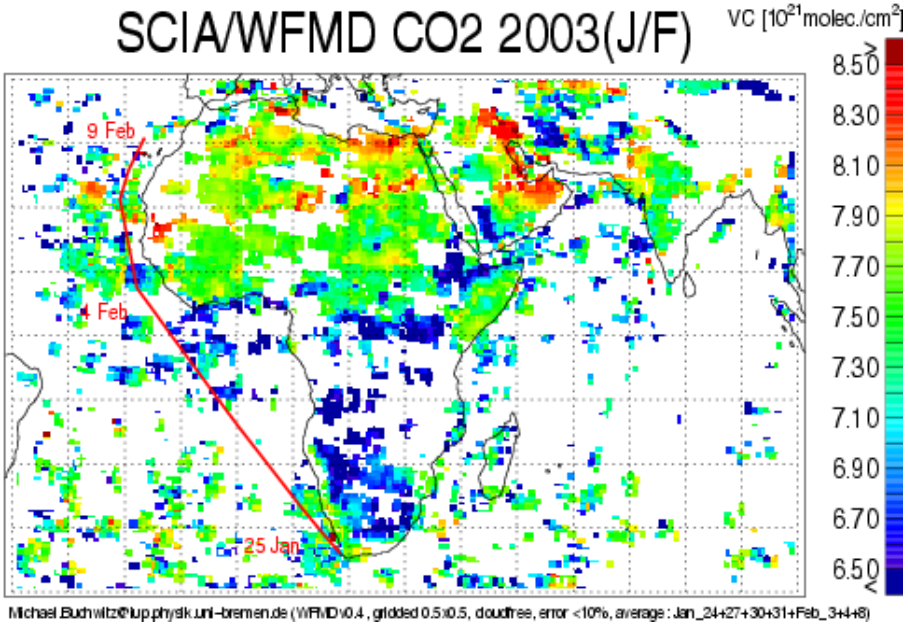

Fig. 22. Similar as Figs. 20 but average over seven days in the time period end of January/beginning of February 2003. The red lines show the ship track of the Polarstern research vessel with an FTS on board for the validation of the SCIAMACHY measurements (see **?**, for details).

ACPD
4, 7217–7279, 2004

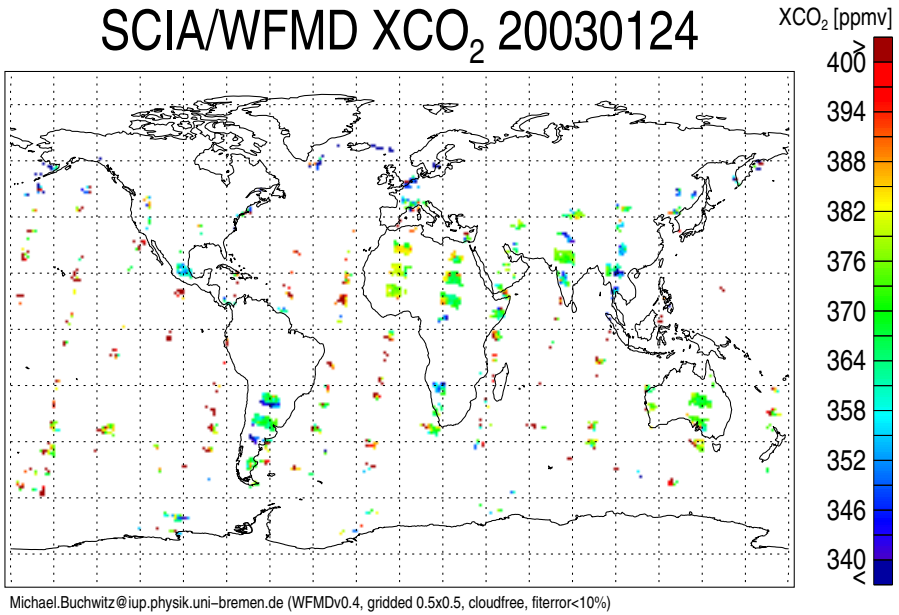

Fig. 23. As Fig. 20 but for XCO_2.

ACPD
4, 7217–7279, 2004

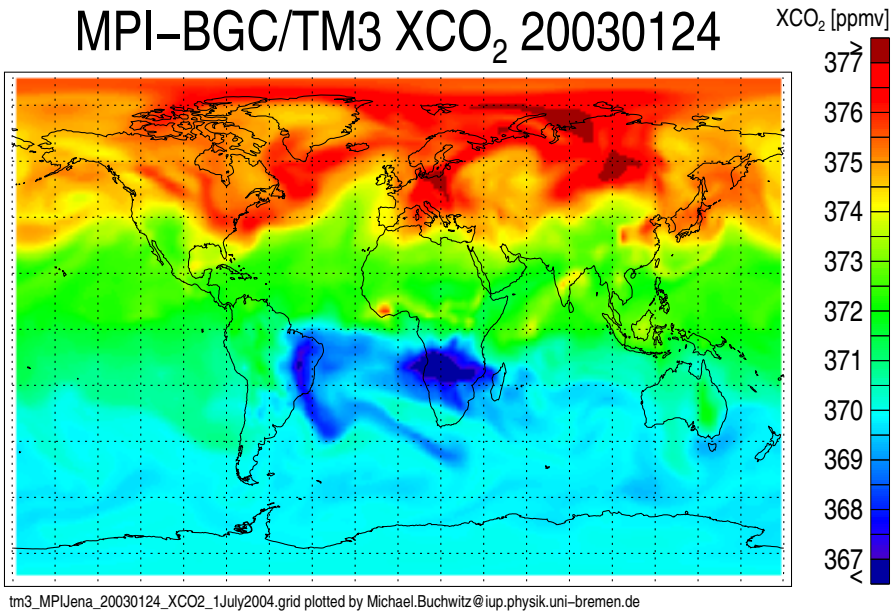

Fig. 24. As Fig. 21 but for XCO_2.

ACPD
4, 7217–7279, 2004

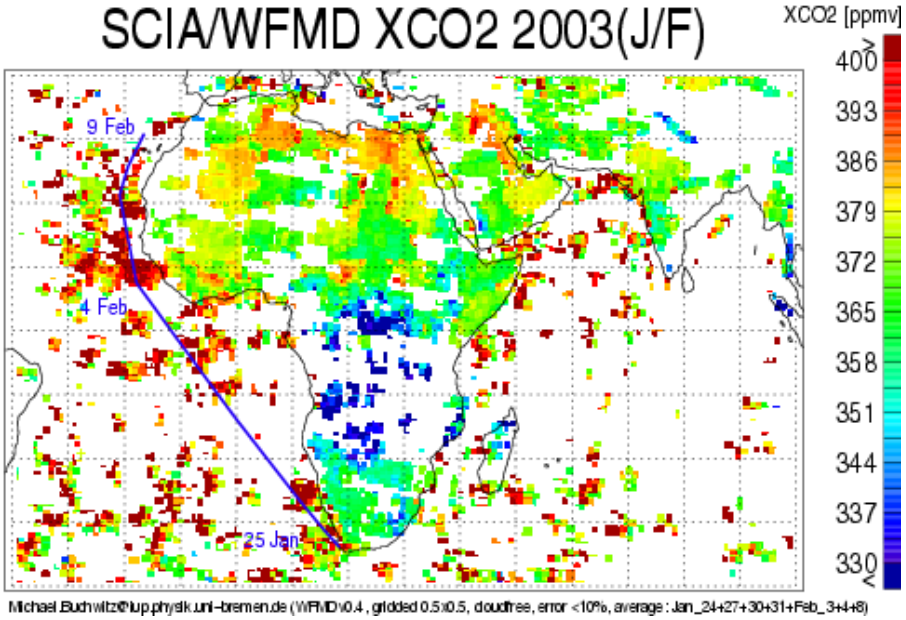

Fig. 25. As Fig. 22 but for XCO_2.

ACPD
4, 7217–7279, 2004

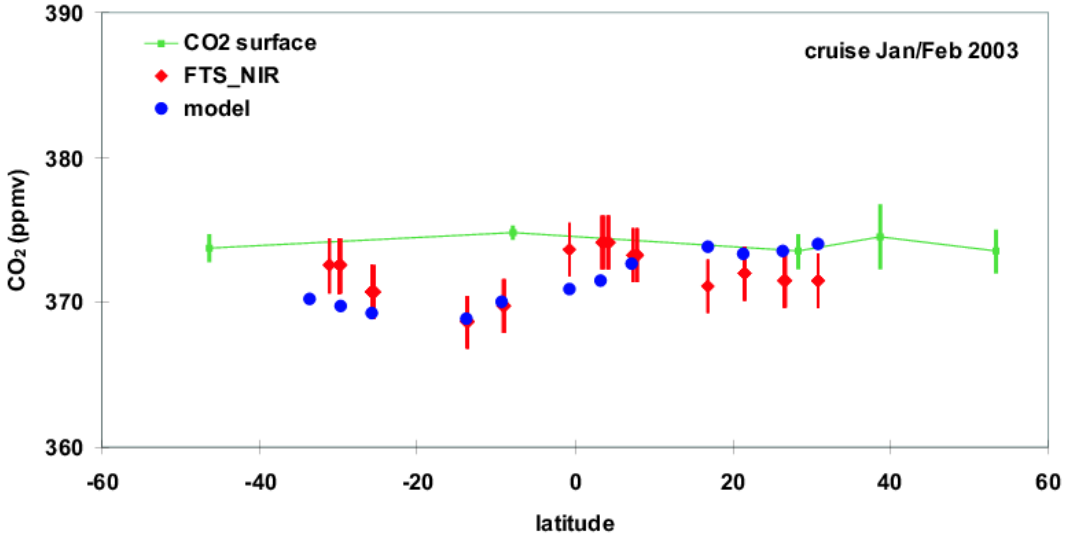

Fig. 26. Column averaged CO_2 mixing ratios (red) measured by Fourier Transform Spectroscopy (FTS) during a ship cruise on the Atlantic in January/February 2003 (**?**). The ship track is shown in Figs. 22 and 25. The corresponding MPI-BGC/TM3 XCO_2 model data are shown in blue. In-situ surface sampling data performed by NOAA/CMDL at ground stations close to the cruise track are shown as green symbols (connected by a green line). The surface stations are: Mace Head, Terceira Island, Tenerife Island, Ascension, and Crozet Island. The green vertical bars indicate the variation of surface CO_2 mixing ratio over the time of the cruise at each station.

ACPD
4, 7217–7279, 2004

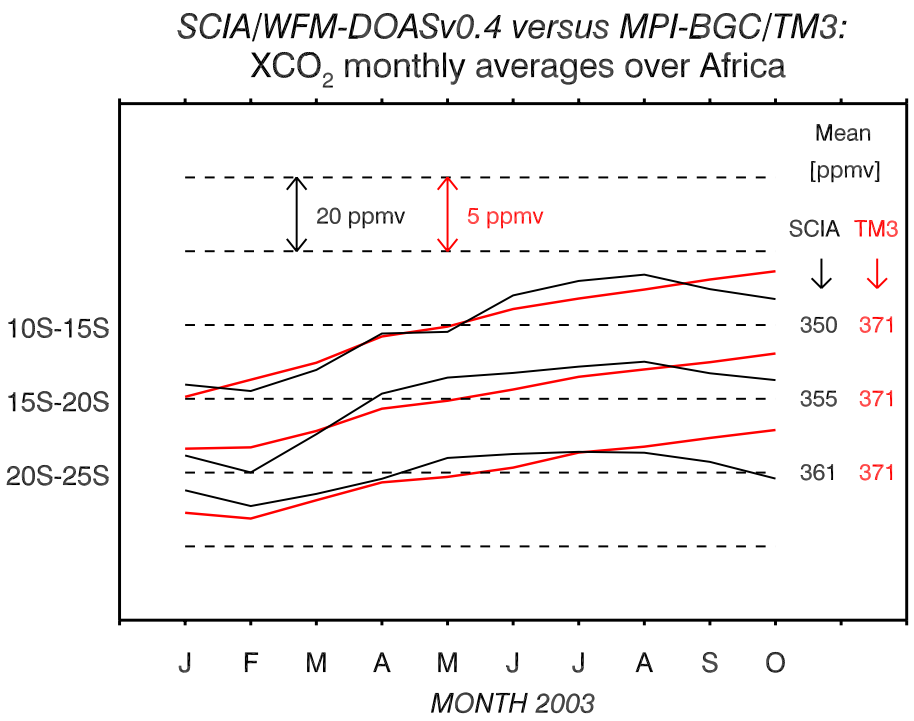

Fig. 27. Monthly mean XCO_2 as measured by SCIAMACHY (black lines) determined by averaging data from all available orbits in three 5° latitude bands over Africa. Only cloud free ground pixels have been considered. The first of the three curves, for example, shows the monthly average XCO_2 values for the latitude interval 10° S–15° S. The average value for this interval is 350 ppmv (see value given on the right hand side). The mixing ratio difference between the dotted horizontal lines is 20 ppmv. From this it can be seen that the XCO_2 in the 10° S–15° S latitude band is about (350-18=) 332 ppmv for February and about (350+13=) 363 ppmv for July 2003. The corresponding MPI-BGC/TM3 model data are shown in red.

ACPD
4, 7217–7279, 2004

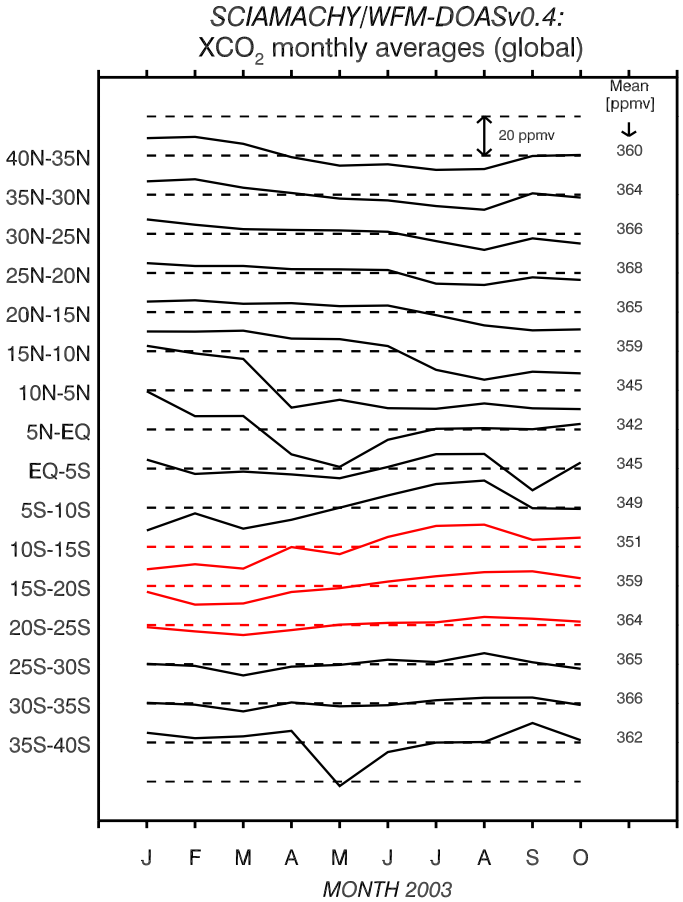

Fig. 28. As Fig. 27 but for global (i.e. not restricted to Africa) year 2003 data including an extended range of latitudes. The three latitudes ranges also shown in Fig. 27 are shown in red. The distance between the dashed horizontal lines corresponds to 20 ppmv.

ACPD
4, 7217–7279, 2004

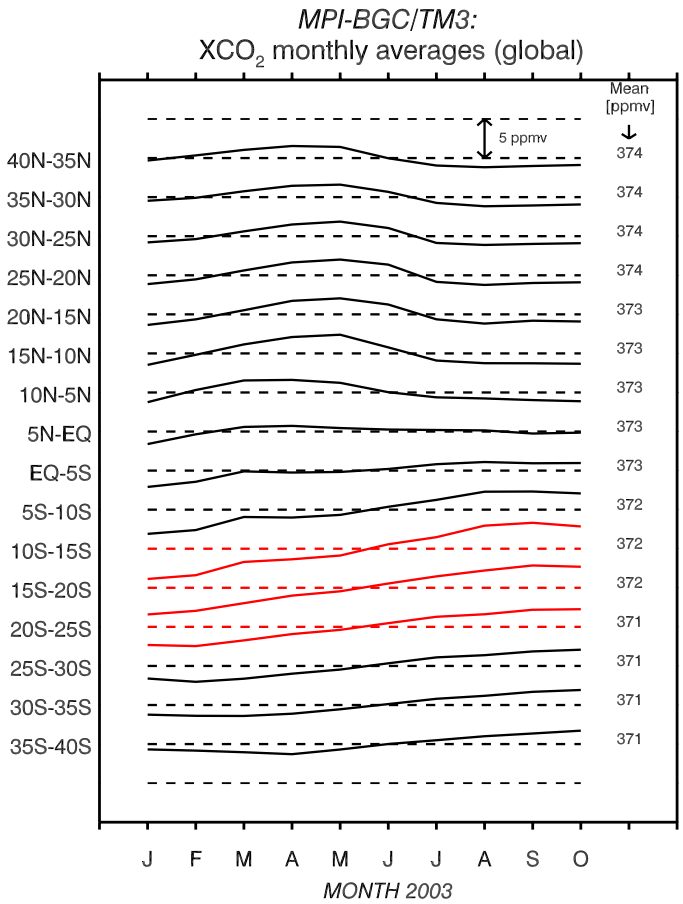

Fig. 29. As Fig. 28 but for the MPI-BGC/TM3 model. The averages have been calculated using all model data over land in the corresponding latitude bands. The distance between the dashed horizontal lines corresponds to 5 ppmv.

ACPD
4, 7217–7279, 2004